but they may have distinct genetic alterations, as observed in the characteristic occurrence of H-*ras* mutations in MNU-induced cancer and LOH regions in PhIP-induced cancer. The existence of indirect effects of carcinogens is suggested for both ionizing radiation and MNU models, though the identity of these indirect effects is uncertain. Estrogens may play a crucial role in the development of cancer in both radiation and chemical models, but the protective effect of parity seems weaker for radiation. Specifically, ionizing radiation may have a strong impact on cancer initiation in a lactating gland. Though only partial evidence is available, ionizing radiation and some chemical carcinogens such as MNU may target stem/progenitor cells located at the TEB or throughout the gland. We perceive that the animal model of radiation carcinogenesis will continue to play a crucial role in bridging results of in vivo animal experiments and observations from human studies and translate into a better understanding of mammary carcinogenesis.

ACKNOWLEDGMENTS

The authors thank E. Obara, Y. Amasaki, Y. Nishimura, J. Nagai, H. Moritake, H. Osada, M. Ootawara, S. Sasaki, and other lab members for technical and secretarial assistance, and the Laboratory Animal Sciences Section for animal management. This research was supported in part by a Grant-In-Aid for Young Scientists (B) from MEXT (No. 20710049), the Third-Term Comprehensive Strategy for Cancer Control (No. 19141201), and a Grant-In-Aid for Cancer Research (No. 19S-1) from the Ministry of Health, Labor and Welfare of Japan.

REFERENCES

1. Thompson, D. E., Mabuchi, K., Ron, E., Soda, M., Tokunaga, M., Ochikubo, S., Sugimoto, S., Ikeda, T., Terasaki, M., Izumi, S., *et al.* (1994) Cancer incidence in atomic bomb survivors. Part II: Solid tumors, 1958–1987. Radiat. Res. **137**: S17–S67.
2. Ronckers, C. M., Erdmann, C. A. and Land, C. E. (2004) Radiation and breast cancer: a review of current evidence. Breast Cancer Res. **7**: 21–32.
3. Preston, D. L., Mattsson, A., Holmberg, E., Shore, R., Hildreth, N. G. and Boice, J. D. J. (2002) Radiation effects on breast cancer risk: a pooled analysis of eight cohorts. Radiat. Res. **158**: 220–235.
4. Preston, D. L., Ron, E., Tokuoka, S., Funamoto, S., Nishi, N., Soda, M., Mabuchi, K. and Kodama, K. (2007) Solid cancer incidence in atomic bomb survivors: 1958–1998. Radiat. Res. **168**: 1–64.
5. Broerse, J. J., van Bekkum, D. W., Zoetelief, J. and Zurcher, C. (1991) Relative biological effectiveness for neutron carcinogenesis in monkeys and rats. Radiat. Res. **128**: S128–S135.
6. Luz, A., Muller, W. A., Linzner, U., Strauss, P. G., Schmidt, J., Muller, K., Atkinson, M. J., Murray, A. B., Gossner, W., Erfle, V., *et al.* (1991) Bone tumor induction after incorporation of short-lived radionuclides. Radiat. Environ Biophys **30**: 225–227.
7. Medina, D. and Thompson, H. J. (2000) A comparison of the salient features of mouse, rat, and human mammary tumorigenesis. In Methods in mammary gland biology and breast cancer research, (Eds.) Ip, M. M. and Asch, B. B., pp. 31–36. Kluwer Academic/Plenum Publishers, New York.
8. Medina, D. (2000) Mouse models for mammary cancer. In Methods in mammary gland biology and breast cancer research, (Eds.) Ip, M. M. and Asch, B. B., pp. 3–17. Kluwer Academic/Plenum Publishers, New York.
9. Thompson, H. J. and Singh, M. (2000) Rat models of premalignant breast disease. J. Mammary Gland Biol. Neoplasia **5**: 409–420.
10. Nandi, S., Guzman, R. C. and Yang, J. (1995) Hormones and mammary carcinogenesis in mice, rats, and humans: a unifying hypothesis. Proc. Natl. Acad. Sci. U. S. A. **92**: 3650–3657.
11. Gould, M. N. (1995) Rodent models for the study of etiology, prevention and treatment of breast cancer. Semin Cancer Biol. **6**: 147–152.
12. Finerty, J. C., Binhammer, R. T., Schneider, M. and Cunningham, A. W. (1953) Neoplasms in rats exposed to single-dose total-body X radiation. J. Natl. Cancer Inst. **14**: 149–157.
13. Shellabarger, C. J., Cronkite, E. P., Bond, V. P. and Lippincott, S. W. (1957) The occurrence of mammary tumors in the rat after sublethal whole-body irradiation. Radiat. Res. **6**: 501–512.
14. Jacrot, M., Mouriquand, J., Mouriquand, C. and Saez, S. (1979) Mammary carcinogenesis in Sprague-Dawley rats following 3 repeated exposures to 14. 8 MeV neutrons and steroid receptor content of these tumor types. Cancer Lett. **8**: 147–153.
15. Welsch, C. W., Goodrich-Smith, M., Brown, C. K., Miglorie, N. and Clifton, K. H. (1981) Effect of an estrogen antagonist (tamoxifen) on the initiation and progression of gamma-irradiation-induced mammary tumors in female Sprague-Dawley rats. Eur. J. Cancer Clin. Oncol. **17**: 1255–1258.
16. Gragtmans, N. J., Myers, D. K., Johnson, J. R., Jones, A. R. and Johnson, L. D. (1984) Occurrence of mammary tumors in rats after exposure to tritium beta rays and 200-kVp X rays. Radiat. Res. **99**: 636–650.
17. Mandybur, T. I., Ormsby, I., Samuels, S. and Mancardi, G. L. (1985) Neural, pituitary, and mammary tumors in Sprague-Dawley rats treated with X irradiation to the head and *N*-ethyl-*N*-nitrosourea (ENU) during the early postnatal period: a statistical study of tumor incidence and survival. Radiat. Res. **101**: 460–472.
18. Lemon, H. M., Kumar, P. F., Peterson, C., Rodriguez-Sierra, J. F. and Abbo, K. M. (1989) Inhibition of radiogenic mammary carcinoma in rats by estriol or tamoxifen. Cancer **63**: 1685–1692.
19. Kantorowitz, D. A., Thompson, H. J. and Furmanski, P. (1995) Effect of high-dose, fractionated local irradiation on MNU-induced carcinogenesis in the rat mammary gland.

Carcinogenesis **16**: 649–653.
20. Haag, J. D., Hsu, L. C., Newton, M. A. and Gould, M. N. (1996) Allelic imbalance in mammary carcinomas induced by either 7,12-dimethylbenz[a]anthracene or ionizing radiation in rats carrying genes conferring differential susceptibilities to mammary carcinogenesis. Mol. Carcinog **17**: 134–143.
21. Bartstra, R. W., Bentvelzen, P. A., Zoetelief, J., Mulder, A. H., Broerse, J. J. and van Bekkum, D. W. (1998) Induction of mammary tumors in rats by single-dose gamma irradiation at different ages. Radiat. Res. **150**: 442–450.
22. Inano, H., Suzuki, K., Ishii-Ohba, H., Ikeda, K. and Wakabayashi, K. (1991) Pregnancy-dependent initiation in tumorigenesis of Wistar rat mammary glands by ^{60}Co-irradiation. Carcinogenesis **12**: 1085–1090.
23. Shellabarger, C. J. (1972) Mammary neoplastic response of Lewis and Sprague-Dawley female rats to 7,12-dimethylbenz(a)anthracene or x-ray. Cancer Res. **32**: 883–885.
24. Holtzman, S., Stone, J. P. and Shellabarger, C. J. (1979) Synergism of diethylstilbestrol and radiation in mammary carcinogenesis in female F344 rats. J. Natl. Cancer Inst. **63**: 1071–1074.
25. Clifton, K. H., Yasukawa-Barnes, J., Tanner, M. A. and Haning, R. V. Jr. (1985) Irradiation and prolactin effects on rat mammary carcinogenesis: intrasplenic pituitary and estrone capsule implants. J. Natl. Cancer Inst. **75**: 167–175.
26. Vogel, H. H. Jr. and Turner, J. E. (1982) Genetic component in rat mammary carcinogenesis. Radiat. Res. **89**: 264–273.
27. Shellabarger, C. J. (1976) Modifying factors in rat mammary gland carcinogenesis. In Biology of Radiation Carcinogenesis, (Eds.) Yuhas, J. M., Tennant, R. W. and Regan, J. D., pp. 31–43. Raven Press, New York.
28. Shellabarger, C. J., Stone, J. P. and Holtzman, S. (1978) Rat differences in mammary tumor induction with estrogen and neutron radiation. J. Natl. Cancer Inst. **61**: 1505–1508.
29. Imaoka, T., Nishimura, M., Kakinuma, S., Hatano, Y., Ohmachi, Y., Kawano, A., Maekawa, A. and Shimada, Y. (2007) High relative biologic effectiveness of carbon ion radiation on induction of rat mammary carcinoma and its lack of H-*ras* and *Tp53* mutations. Int. J. Radiat. Oncol. Biol. Phys. **69**: 194–203.
30. Holtzman, S., Stone, J. P. and Shellabarger, C. J. (1981) Synergism of estrogens and X-rays in mammary carcinogenesis in female ACI rats. J. Natl. Cancer Inst. **67**: 455–459.
31. Ullrich, R. L. and Preston, R. J. (1991) Radiation induced mammary cancer. J. Radiat. Res. (Tokyo) **32 Suppl 2**: 104–109.
32. Yu, Y., Okayasu, R., Weil, M. M., Silver, A., McCarthy, M., Zabriskie, R., Long, S., Cox, R. and Ullrich, R. L. (2001) Elevated breast cancer risk in irradiated BALB/c mice associates with unique functional polymorphism of the *Prkdc* (DNA-dependent protein kinase catalytic subunit) gene. Cancer Res. **61**: 1820–1824.
33. Mori, N., Yamate, J., Umesako, S., Hong, D. P., Okumoto, M. and Nakao, R. (2003) Preferential induction of mammary tumors in p53 hemizygous BALB/c mice by fractionated irradiation of a sub-lethal dose of X-rays. J. Radiat. Res. (Tokyo) **44**: 249–254.
34. Backlund, M. G., Trasti, S. L., Backlund, D. C., Cressman, V. L., Godfrey, V. and Koller, B. H. (2001) Impact of ionizing radiation and genetic background on mammary tumorigenesis in *p53*-deficient mice. Cancer Res. **61**: 6577–6582.
35. Umesako, S., Fujisawa, K., Iiga, S., Mori, N., Takahashi, M., Hong, D. P., Song, C. W., Haga, S., Imai, S., Niwa, O. and Okumoto, M. (2005) *Atm* heterozygous deficiency enhances development of mammary carcinomas in *p53* heterozygous knockout mice. Breast Cancer Res. **7**: R164–R170.
36. Cressman, V. L., Backlund, D. C., Hicks, E. M., Gowen, L. C., Godfrey, V. and Koller, B. H. (1999) Mammary tumor formation in *p53*- and *BRCA1*-deficient mice. Cell Growth Differ **10**: 1–10.
37. van der Houven van Oordt, C. W., Smits, R., Schouten, T. G., Houwing-Duistermaat, J. J., Williamson, S. L., Luz, A., Meera Khan, P., van der Eb, A. J., Breuer, M. L. and Fodde, R. (1999) The genetic background modifies the spontaneous and X-ray-induced tumor spectrum in the Apc1638N mouse model. Genes Chromosomes Cancer **24**: 191–198.
38. Imaoka, T., Okamoto, M., Nishimura, M., Nishimura, Y., Ootawara, M., Kakinuma, S., Tokairin, Y. and Shimada, Y. (2006) Mammary tumorigenesis in $Apc^{Min/+}$ mice is enhanced by X-irradiation with a characteristic age dependence. Radiat. Res. **165**: 165–173.
39. Ullrich, R. L., Jernigan, M. C. and Storer, J. B. (1977) Neutron carcinogenesis. Dose and dose-rate effects in BALB/c mice. Radiat. Res. **72**: 487–498.
40. Ullrich, R. L. (1983) Tumor induction in BALB/c female mice after fission neutron or gamma irradiation. Radiat. Res. **93**: 506–515.
41. Ullrich, R. L. (1984) Tumor induction in BALB/c mice after fractionated or protracted exposures to fission-spectrum neutrons. Radiat. Res. **97**: 587–597.
42. Dicello, J. F., Christian, A., Cucinotta, F. A., Gridley, D. S., Kathirithamby, R., Mann, J., Markham, A. R., Moyers, M. F., Novak, G. R., Piantadosi, S., Ricart-Arbona, R., Simonson, D. M., Strandberg, J. D., Vazquez, M., Williams, J. R., Zhang, Y., Zhou, H. and Huso, D. (2004) In vivo mammary tumourigenesis in the Sprague-Dawley rat and microdosimetric correlates. Phys. Med. Biol. **49**: 3817–3830.
43. Shellabarger, C. J., Baum, J. W., Holtzman, S. and Stone, J. P. (1985) Neon-20 ion- and X-ray-induced mammary carcinogenesis in female rats. Ann. N. Y. Acad. Sci. **459**: 239–244.
44. Sanders, C. L. Jr. (1974) Rat mammary neoplasia following deposition of plutonium. Health Phys. **27**: 592–593.
45. Russo, J., Russo, I. H., Rogers, A. E., van Zwieten, M. J. and Gusterson, B. (1990) Tumor of the mammary gland. In Pahology of Tumours in Laboratory Animals Volume 1 - Tumours of the Rat, 2nd Ed. edition, (Eds.) Turusov, V. and Mohr, U., pp. 47–78. IARC Scientific Publications, Lyon.
46. Nagao, M., Ushijima, T., Watanabe, N., Okochi, E., Ochiai, M., Nakagama, H. and Sugimura, T. (2002) Studies on mammary carcinogenesis induced by a heterocyclic amine, 2-amino-1-methyl-6-phenylimidazo[4,5-b]pyridine, in mice and rats. Environ Mol. Mutagen **39**: 158–164.
47. Russo, J. and Russo, I. H. (2000) Atlas and histologic classification of tumors of the rat mammary gland. J. Mammary

Gland Biol. Neoplasia **5**: 187–200.
48. Tsubura, A., Yoshizawa, K., Uehara, N., Yuri, T. and Matsuoka, Y. (2007) Multistep mouse mammary tumorigenesis through pre-neoplasia to neoplasia and acquisition of metastatic potential. Med. Mol. Morphol **40**: 9–17.
49. Shellabarger, C. J., Bond, V. P. and Cronkite, E. P. (1960) Studies on radiation-induced mammary gland neoplasia in the rat. 4. The response of females to a single dose of sublethal total-body gamma radiation as studied until the first appearance of breast neoplasia or death of the animals. Radiat. Res. **13**: 242–249.
50. Humphreys, R. C., Krajewska, M., Krnacik, S., Jaeger, R., Weiher, H., Krajewski, S., Reed, J. C. and Rosen, J. M. (1996) Apoptosis in the terminal endbud of the murine mammary gland: a mechanism of ductal morphogenesis. Development **122**: 4013–4022.
51. Russo, J., Tay, L. K. and Russo, I. H. (1982) Differentiation of the mammary gland and susceptibility to carcinogenesis. Breast Cancer Res. Treat. **2**: 5–73.
52. Korkola, J. E. and Archer, M. C. (1999) Resistance to mammary tumorigenesis in Copenhagen rats is associated with the loss of preneoplastic lesions. Carcinogenesis **20**: 221–227.
53. Osborne, M. P., Ruperto, J. F., Crowe, J. P., Rosen, P. P. and Telang, N. T. (1992) Effect of tamoxifen on preneoplastic cell proliferation in *N*-nitroso-*N*-methylurea-induced mammary carcinogenesis. Cancer Res. **52**: 1477–1480.
54. Shilkaitis, A., Green, A., Steele, V., Lubet, R., Kelloff, G. and Christov, K. (2000) Neoplastic transformation of mammary epithelial cells in rats is associated with decreased apoptotic cell death. Carcinogenesis **21**: 227–233.
55. Imaoka, T., Nishimura, M., Nishimura, Y., Kakinuma, S. and Shimada, Y. (2006) Persistent cell proliferation of terminal end buds precedes radiation-induced rat mammary carcinogenesis. In Vivo **20**: 353–358.
56. Sharkey, S. M. and Bruce, W. R. (1986) Quantitation of nuclear aberrations as a screen for agents damaging to mammary epithelium. Carcinogenesis **7**: 1991–1995.
57. Faulkin, L. J. Jr., Shellabarger, C. J. and DeOme, K. B. (1967) Hyperplastic lesions of Sprague-Dawley rat mammary glands after X irradiation. J. Natl. Cancer Inst. **39**: 449–458.
58. Ponomareva, O. N., Rose, J. A., Lasarev, M., Rasey, J. and Turker, M. S. (2002) Tissue-specific deletion and discontinuous loss of heterozygosity are signatures for the mutagenic effects of ionizing radiation in solid tissues. Cancer Res. **62**: 1518–1523.
59. Nohmi, T. and Masumura, K. (2005) Molecular nature of intrachromosomal deletions and base substitutions induced by environmental mutagens. Environ Mol. Mutagen **45**: 150–161.
60. Sukumar, S., Notario, V., Martin-Zanca, D. and Barbacid, M. (1983) Induction of mammary carcinomas in rats by nitrosomethylurea involves malignant activation of H-ras-1 locus by single point mutations. Nature **306**: 658–661.
61. Hokaiwado, N., Asamoto, M., Cho, Y. M., Imaida, K. and Shirai, T. (2001) Frequent c-Ha-ras gene mutations in rat mammary carcinomas induced by 2-amino-1-methyl-6-phenylimidazo[4,5-b]pyridine. Cancer Lett. **163**: 187–190.
62. Ushijima, T., Kakiuchi, H., Makino, H., Hasegawa, R., Ishizaka, Y., Hirai, H., Yazaki, Y., Ito, N., Sugimura, T. and Nagao, M. (1994) Infrequent mutation of Ha-ras and p53 in rat mammary carcinomas induced by 2-amino-1-methyl-6-phenylimidazo[4,5-b]pyridine. Mol. Carcinog **10**: 38–44.
63. Yu, M. and Snyderwine, E. G. (2002) H-*ras* oncogene mutations during development of 2-amino-1-methyl-6-phenylimidazo[4,5-b]pyridine (PhIP)-induced rat mammary gland cancer. Carcinogenesis **23**: 2123–2128.
64. Waldmann, V., Suchy, B. and Rabes, H. M. (1993) Cell proliferation and prevalence of ras gene mutations in 7,12-dimethylbenz(a)anthracene (DMBA)-induced rat mammary tumors. Res. Exp. Med. (Berl) **193**: 143–151.
65. Imaoka, T., Nishimura, M., Teramoto, A., Nishimura, Y., Ootawara, M., Osada, H., Kakinuma, S., Maekawa, A. and Shimada, Y. (2005) Cooperative induction of rat mammary cancer by radiation and 1-methyl-1-nitrosourea via the oncogenic pathways involving c-Myc activation and H-*ras* mutation. Int. J. Cancer **115**: 187–193.
66. Toyota, M., Ushijima, T., Weisburger, J. H., Hosoya, Y., Canzian, F., Rivenson, A., Imai, K., Sugimura, T. and Nagao, M. (1996) Microsatellite instability and loss of heterozygosity on chromosome 10 in rat mammary tumors induced by 2-amino-1-methyl-6-phenylimidazo[4,5-b]pyridine. Mol. Carcinog **15**: 176–182.
67. Yu, M., Ryu, D. Y. and Snyderwine, E. G. (2000) Genomic imbalance in rat mammary gland carcinomas induced by 2-amino-1-methyl-6-phenylimidazo(4,5-b)pyridine. Mol. Carcinog **27**: 76–83.
68. Haag, J. D., Brasic, G. M., Shepel, L. A., Newton, M. A., Grubbs, C. J., Lubet, R. A., Kelloff, G. J. and Gould, M. N. (1999) A comparative analysis of allelic imbalance events in chemically induced rat mammary, colon, and bladder tumors. Mol. Carcinog **24**: 47–56.
69. Shimada, Y., Nishimura, M., Kakinuma, S., Okumoto, M., Shiroishi, T., Clifton, K. H. and Wakana, S. (2000) Radiation-associated loss of heterozygosity at the *Znfn1a1* (*Ikaros*) locus on chromosome 11 in murine thymic lymphomas. Radiat. Res. **154**: 293–300.
70. Yoshida, M. A., Nakata, A., Akiyama, M., Kakinuma, S., Sado, T., Nishimura, M. and Shimada, Y. (2007) Distinct structural abnormalities of chromosomes 11 and 12 associated with loss of heterozygosity in X-ray-induced mouse thymic lymphomas. Cancer Genet. Cytogenet **179**: 1–10.
71. Christian, A. T., Snyderwine, E. G. and Tucker, J. D. (2002) Comparative genomic hybridization analysis of PhIP-induced mammary carcinomas in rats reveals a cytogenetic signature. Mutat. Res. **506–507**: 113–119.
72. Imaoka, T., Yamashita, S., Nishimura, M., Kakinuma, S., Ushijima, T. and Shimada, Y. (2008) Gene expression profiling distinguishes between spontaneous and radiation-induced rat mammary carcinomas. J. Radiat. Res. (Tokyo) **49**: 349–360.
73. Chan, M. M., Lu, X., Merchant, F. M., Iglehart, J. D. and Miron, P. L. (2005) Gene expression profiling of NMU-induced rat mammary tumors: cross species comparison with human breast cancer. Carcinogenesis **26**: 1343–1353.

74. Shan, L., Yu, M. and Snyderwine, E. G. (2005) Gene expression profiling of chemically induced rat mammary gland cancer. Carcinogenesis **26**: 503–509.
75. Shan, L., He, M., Yu, M., Qiu, C., Lee, N. H., Liu, E. T. and Snyderwine, E. G. (2002) cDNA microarray profiling of rat mammary gland carcinomas induced by 2-amino-1-methyl-6-phenylimidazo[4,5-b]pyridine and 7,12-dimethylbenz[a] anthracene. Carcinogenesis **23**: 1561–1568.
76. Kuramoto, T., Morimura, K., Yamashita, S., Okochi, E., Watanabe, N., Ohta, T., Ohki, M., Fukushima, S., Sugimura, T. and Ushijima, T. (2002) Etiology-specific gene expression profiles in rat mammary carcinomas. Cancer Res. **62**: 3592–3597.
77. Lee, H. J., Lee, Y. J., Kang, C. M., Bae, S., Jeoung, D., Jang, J. J., Lee, S. S., Cho, C. K. and Lee, Y. S. (2008) Differential gene signatures in rat mammary tumors induced by DMBA and those induced by fractionated gamma radiation. Radiat. Res. **170**: 579–590.
78. Tsai, K. K., Chuang, E. Y., Little, J. B. and Yuan, Z. M. (2005) Cellular mechanisms for low-dose ionizing radiation-induced perturbation of the breast tissue microenvironment. Cancer Res. **65**: 6734–6744.
79. Barcellos-Hoff, M. H. and Ravani, S. A. (2000) Irradiated mammary gland stroma promotes the expression of tumorigenic potential by unirradiated epithelial cells. Cancer Res. **60**: 1254–1260.
80. Barcellos-Hoff, M. H., Derynck, R., Tsang, M. L. and Weatherbee, J. A. (1994) Transforming growth factor-beta activation in irradiated murine mammary gland. J. Clin. Invest **93**: 892–899.
81. Ehrhart, E. J., Segarini, P., Tsang, M. L., Carroll, A. G. and Barcellos-Hoff, M. H. (1997) Latent transforming growth factor beta1 activation in situ: quantitative and functional evidence after low-dose gamma-irradiation. FASEB J. **11**: 991–1002.
82. Ewan, K. B., Henshall-Powell, R. L., Ravani, S. A., Pajares, M. J., Arteaga, C., Warters, R., Akhurst, R. J. and Barcellos-Hoff, M. H. (2002) Transforming growth factor-beta1 mediates cellular response to DNA damage in situ. Cancer Res. **62**: 5627–5631.
83. Andarawewa, K. L., Erickson, A. C., Chou, W. S., Costes, S. V., Gascard, P., Mott, J. D., Bissell, M. J. and Barcellos-Hoff, M. H. (2007) Ionizing radiation predisposes nonmalignant human mammary epithelial cells to undergo transforming growth factor beta induced epithelial to mesenchymal transition. Cancer Res. **67**: 8662–8670.
84. Maffini, M. V., Soto, A. M., Calabro, J. M., Ucci, A. A. and Sonnenschein, C. (2004) The stroma as a crucial target in rat mammary gland carcinogenesis. J. Cell Sci. **117**: 1495–1502.
85. Medina, D. and Kittrell, F. (2005) Stroma is not a major target in DMBA-mediated tumorigenesis of mouse mammary preneoplasia. J. Cell Sci. **118**: 123–127.
86. Kelsey, J. L. and Berkowitz, G. S. (1988) Breast cancer epidemiology. Cancer Res. **48**: 5615–5623.
87. Goodman, M. T., Cologne, J. B., Moriwaki, H., Vaeth, M. and Mabuchi, K. (1997) Risk factors for primary breast cancer in Japan: 8-year follow-up of atomic bomb survivors. Prev. Med. **26**: 144–153.
88. Yamanouchi, H., Ishii-Ohba, H., Suzuki, K., Onoda, M., Wakabayashi, K. and Inano, H. (1995) Relationship between stages of mammary development and sensitivity to gamma-ray irradiation in mammary tumorigenesis in rats. Int. J. Cancer **60**: 230–234.
89. Inano, H., Yamanouchi, H., Suzuki, K., Onoda, M. and Wakabayashi, K. (1995) Estradiol-17 beta as an initiation modifier for radiation-induced mammary tumorigenesis of rats ovariectomized before puberty. Carcinogenesis **16**: 1871–1877.
90. Knott, K. K., McGinley, J. N., Lubet, R. A., Steele, V. E. and Thompson, H. J. (2001) Effect of the aromatase inhibitor vorozole on estrogen and progesterone receptor content of rat mammary carcinomas induced by 1-methyl-1-nitrosourea. Breast Cancer Res. Treat. **70**: 171–183.
91. Thompson, H. J., McGinley, J., Rothhammer, K. and Singh, M. (1998) Ovarian hormone dependence of pre-malignant and malignant mammary gland lesions induced in prepubertal rats by 1-methyl-1-nitrosourea. Carcinogenesis **19**: 383–386.
92. Ueda, M., Imai, T., Takizawa, T., Onodera, H., Mitsumori, K., Matsui, T. and Hirose, M. (2005) Possible enhancing effects of atrazine on growth of 7,12-dimethylbenz(a) anthracene-induced mammary tumors in ovariectomized Sprague-Dawley rats. Cancer Sci. **96**: 19–25.
93. Thompson, H. J., Meeker, L. D., Tagliaferro, A. R. and Becci, P. J. (1982) Effect of retinyl acetate on the occurrence of ovarian hormone-responsive and -nonresponsive mammary cancers in the rat. Cancer Res. **42**: 903–905.
94. Huggins, C. and Fukunishi, R. (1963) Cancer in the rat after single exposures to irradiation or hydrocarbons. Age and strain factors. Hormone dependence of the mammary cancers. Radiat. Res. **20**: 493–503.
95. Yang, J., Yoshizawa, K., Nandi, S. and Tsubura, A. (1999) Protective effects of pregnancy and lactation against *N*-methyl-*N*-nitrosourea-induced mammary carcinomas in female Lewis rats. Carcinogenesis **20**: 623–628.
96. Sinha, D. K., Pazik, J. E. and Dao, T. L. (1983) Progression of rat mammary development with age and its relationship to carcinogenesis by a chemical carcinogen. Int. J. Cancer **31**: 321–327.
97. Russo, I. H., Koszalka, M. and Russo, J. (1991) Comparative study of the influence of pregnancy and hormonal treatment on mammary carcinogenesis. Br. J. Cancer **64**: 481–484.
98. Abrams, T. J., Guzman, R. C., Swanson, S. M., Thordarson, G., Talamantes, F. and Nandi, S. (1998) Changes in the parous rat mammary gland environment are involved in parity-associated protection against mammary carcinogenesis. Anticancer Res. **18**: 4115–4121.
99. Thordarson, G., Jin, E., Guzman, R. C., Swanson, S. M., Nandi, S. and Talamantes, F. (1995) Refractoriness to mammary tumorigenesis in parous rats: is it caused by persistent changes in the hormonal environment or permanent biochemical alterations in the mammary epithelia? Carcinogenesis **16**: 2847–2853.
100. Sivaraman, L., Stephens, L. C., Markaverich, B. M., Clark, J. A., Krnacik, S., Conneely, O. M., O'Malley, B. W. and Medina, D. (1998) Hormone-induced refractoriness to mam-

mary carcinogenesis in Wistar-Furth rats. Carcinogenesis **19**: 1573–1581.
101. Matsuoka, Y., Fukamachi, K., Uehara, N., Tsuda, H. and Tsubura, A. (2008) Induction of a novel histone deacetylase 1/c-Myc/Mnt/Max complex formation is implicated in parity-induced refractoriness to mammary carcinogenesis. Cancer Sci. **99**: 309–315.
102. Shellabarger, C. J., Aponte, G. E., Cronkite, E. P. and Bond, V. P. (1962) Studies on radiation-induced mammary gland neoplasia in the rat. VI. The effect of changes in thyroid function, ovarian function and pregnancy. Radiat. Res. **17**: 492–507.
103. Holtzman, S., Stone, J. P. and Shellabarger, C. J. (1982) Radiation-induced mammary carcinogenesis in virgin, pregnant, lactating, and postlactating rats. Cancer Res. **42**: 50–53.
104. Inano, H., Suzuki, K., Onoda, M. and Yamanouchi, H. (1996) Susceptibility of fetal, virgin, pregnant and lactating rats for the induction of mammary tumors by gamma rays. Radiat. Res. **145**: 708–713.
105. Land, C. E., Tokunaga, M., Tokuoka, S. and Nakamura, N. (1993) Early-onset breast cancer in A-bomb survivors. Lancet **342**: 237.
106. Land, C. E., Tokunaga, M., Koyama, K., Soda, M., Preston, D. L., Nishimori, I. and Tokuoka, S. (2003) Incidence of female breast cancer among atomic bomb survivors, Hiroshima and Nagasaki, 1950–1990. Radiat. Res. **160**: 707–717.
107. Russo, J., Wilgus, G. and Russo, I. H. (1979) Susceptibility of the mammary gland to carcinogenesis: I Differentiation of the mammary gland as determinant of tumor incidence and type of lesion. Am. J. Pathol. **96**: 721–736.
108. Janss, D. H. and Ben, T. L. (1978) Age-related modification of 7,12-dimethylbenz[a]anthracene binding to rat mammary gland DNA. J. Natl. Cancer Inst. **60**: 173–177.
109. Ariazi, J. L., Haag, J. D., Lindstrom, M. J. and Gould, M. N. (2005) Mammary glands of sexually immature rats are more susceptible than those of mature rats to the carcinogenic, lethal, and mutagenic effects of *N*-nitroso-*N*-methylurea. Mol. Carcinog **43**: 155–164.
110. Grubbs, C. J., Peckham, J. C. and Cato, K. D. (1983) Mammary carcinogenesis in rats in relation to age at time of *N*-nitroso-*N*-methylurea administration. J. Natl. Cancer Inst. **70**: 209–212.
111. Ariazi, J. L., Haag, J. D. and Gould, M. N. (2005) Methylguanine methyltransferase activity deficiency in immature rat mammary epithelial cells parallels increased carcinogenic susceptibility. Mol. Carcinog **44**: 193–201.
112. Moser, A. R., Mattes, E. M., Dove, W. F., Lindstrom, M. J., Haag, J. D. and Gould, M. N. (1993) ApcMin, a mutation in the murine Apc gene, predisposes to mammary carcinomas and focal alveolar hyperplasias. Proc. Natl. Acad. Sci. U. S. A. **90**: 8977–8981.
113. Shan, L., Yu, M., Schut, H. A. and Snyderwine, E. G. (2004) Susceptibility of rats to mammary gland carcinogenesis by the food-derived carcinogen 2-amino-1-methyl-6-phenylimidazo[4,5-b]pyridine (PhIP) varies with age and is associated with the induction of differential gene expression. Am. J. Pathol. **165**: 191–202.
114. Kamiya, K., Gould, M. N. and Clifton, K. H. (1991) Differential control of alveolar and ductal development in grafts of monodispersed rat mammary epithelium. Proc. Soc. Exp. Biol. Med. **196**: 284–292.
115. Smith, G. H. (1996) Experimental mammary epithelial morphogenesis in an in vivo model: evidence for distinct cellular progenitors of the ductal and lobular phenotype. Breast Cancer Res. Treat. **39**: 21–31.
116. Kordon, E. C. and Smith, G. H. (1998) An entire functional mammary gland may comprise the progeny from a single cell. Development **125**: 1921–1930.
117. Kim, N. D., Oberley, T. D., Yasukawa-Barnes, J. and Clifton, K. H. (2000) Stem cell characteristics of transplanted rat mammary clonogens. Exp. Cell Res. **260**: 146–159.
118. Gould, M. N. and Clifton, K. H. (1977) The survival of mammary cells following irradiation in vivo: a directly generated single-dose-survival curve. Radiat. Res. **72**: 343–352.
119. Clifton, K. H., Tanner, M. A. and Gould, M. N. (1986) Assessment of radiogenic cancer initiation frequency per clonogenic rat mammary cell in vivo. Cancer Res. **46**: 2390–2395.
120. Kamiya, K., Yasukawa-Barnes, J., Mitchen, J. M., Gould, M. N. and Clifton, K. H. (1995) Evidence that carcinogenesis involves an imbalance between epigenetic high-frequency initiation and suppression of promotion. Proc. Natl. Acad. Sci. U. S. A. **92**: 1332–1336.
121. Stingl, J., Eirew, P., Ricketson, I., Shackleton, M., Vaillant, F., Choi, D., Li, H. I. and Eaves, C. J. (2006) Purification and unique properties of mammary epithelial stem cells. Nature **439**: 993–997.
122. Shackleton, M., Vaillant, F., Simpson, K. J., Stingl, J., Smyth, G. K., Asselin-Labat, M. L., Wu, L., Lindeman, G. J. and Visvader, J. E. (2006) Generation of a functional mammary gland from a single stem cell. Nature **439**: 84–88.
123. Woodward, W. A., Chen, M. S., Behbod, F., Alfaro, M. P., Buchholz, T. A. and Rosen, J. M. (2007) WNT/beta-catenin mediates radiation resistance of mouse mammary progenitor cells. Proc. Natl. Acad. Sci. U. S. A. **104**: 618–623.
124. Smith, G. H. and Boulanger, C. A. (2003) Mammary epithelial stem cells: transplantation and self-renewal analysis. Cell Prolif **36 Suppl 1**: 3–15.
125. Smith, G. H. (2005) Label-retaining epithelial cells in mouse mammary gland divide asymmetrically and retain their template DNA strands. Development **132**: 681–687.
126. Booth, B. W. and Smith, G. H. (2006) Estrogen receptor-alpha and progesterone receptor are expressed in label-retaining mammary epithelial cells that divide asymmetrically and retain their template DNA strands. Breast Cancer Res. **8**: R49.
127. Booth, B. W., Boulanger, C. A. and Smith, G. H. (2008) Selective segregation of DNA strands persists in long label retaining mammary cells during pregnancy. Breast Cancer Res. **10**: R90.
128. Welm, B. E., Tepera, S. B., Venezia, T., Graubert, T. A., Rosen, J. M. and Goodell, M. A. (2002) Sca-1$^{(pos)}$ cells in the mouse mammary gland represent an enriched progenitor cell population. Dev. Biol. **245**: 42–56.
129. Shellabarger, C. J., Bond, V. P., Aponte, G. E. and Cronkite,

E. P. (1966) Results of fractionation and protraction of total-body radiation on rat mammary neoplasia. Cancer Res. **26**: 509–513.
130. Bartstra, R. W., Bentvelzen, P. A., Zoetelief, J., Mulder, A. H., Broerse, J. J. and van Bekkum, D. W. (2000) The effects of fractionated gamma irradiation on induction of mammary carcinoma in normal and estrogen-treated rats. Radiat. Res. **153**: 557–569.
131. Broerse, J. J., Hennen, L. A., Klapwijk, W. M. and Solleveld, H. A. (1987) Mammary carcinogenesis in different rat strains after irradiation and hormone administration. Int. J. Radiat. Biol. Relat. Stud. Phys. Chem. Med. **51**: 1091–1100.
132. Asselin-Labat, M. L., Shackleton, M., Stingl, J., Vaillant, F., Forrest, N. C., Eaves, C. J., Visvader, J. E. and Lindeman, G. J. (2006) Steroid hormone receptor status of mouse mammary stem cells. J. Natl. Cancer Inst. **98**: 1011–1014.
133. Sleeman, K. E., Kendrick, H., Robertson, D., Isacke, C. M., Ashworth, A. and Smalley, M. J. (2007) Dissociation of estrogen receptor expression and in vivo stem cell activity in the mammary gland. J. Cell Biol. **176**: 19–26.
134. Sorlie, T., Perou, C. M., Tibshirani, R., Aas, T., Geisler, S., Johnsen, H., Hastie, T., Eisen, M. B., van de Rijn, M., Jeffrey, S. S., Thorsen, T., Quist, H., Matese, J. C., Brown, P. O., Botstein, D., Eystein Lonning, P. and Borresen-Dale, A. L. (2001) Gene expression patterns of breast carcinomas distinguish tumor subclasses with clinical implications. Proc. Natl. Acad. Sci. U. S. A. **98**: 10869–10874.
135. Castiglioni, F., Terenziani, M., Carcangiu, M. L., Miliano, R., Aiello, P., Bertola, L., Triulzi, T., Gasparini, P., Camerini, T., Sozzi, G., Fossati-Bellani, F., Menard, S. and Tagliabue, E. (2007) Radiation effects on development of HER2-positive breast carcinomas. Clin. Cancer Res. **13**: 46–51.
136. Saal, L. H., Gruvberger-Saal, S. K., Persson, C., Lovgren, K., Jumppanen, M., Staaf, J., Jonsson, G., Pires, M. M., Maurer, M., Holm, K., Koujak, S., Subramaniyam, S., Vallon-Christersson, J., Olsson, H., Su, T., Memeo, L., Ludwig, T., Ethier, S. P., Krogh, M., Szabolcs, M., Murty, V. V., Isola, J., Hibshoosh, H., Parsons, R. and Borg, A. (2008) Recurrent gross mutations of the *PTEN* tumor suppressor gene in breast cancers with deficient DSB repair. Nat. Genet. **40**: 102–107.
137. Liu, X., Holstege, H., van der Gulden, H., Treur-Mulder, M., Zevenhoven, J., Velds, A., Kerkhoven, R. M., van Vliet, M. H., Wessels, L. F., Peterse, J. L., Berns, A. and Jonkers, J. (2007) Somatic loss of BRCA1 and p53 in mice induces mammary tumors with features of human BRCA1-mutated basal-like breast cancer. Proc. Natl. Acad. Sci. U. S. A. **104**: 12111–12116.
138. McCarthy, A., Savage, K., Gabriel, A., Naceur, C., Reis-Filho, J. S. and Ashworth, A. (2007) A mouse model of basal-like breast carcinoma with metaplastic elements. J. Pathol. **211**: 389–398.

Received on March 11, 2009
Accepted on April 29, 2009
J-STAGE Advance Publication Date: June 9, 2009

RADIATION RESEARCH 173, 310–318 (2010)
0033-7587/10 $15.00

DOI: 10.1667/RR1905.1

Unique Characteristics of Radiation-Induced Apoptosis in the Postnatally Developing Small Intestine and Colon of Mice

T. Miyoshi-Imamura,[a,b] S. Kakinuma,[b] M. Kaminishi,[b] M. Okamoto,[b] T. Takabatake,[b] Y. Nishimura,[b] T. Imaoka,[b] M. Nishimura,[b] K. Murakami-Murofushi[a] and Y. Shimada[b,1]

[a] *Genetic Counseling Program, Graduate School of Humanities and Sciences, Ochanomizu University, 2-1-1 Otsuka, Bunkyo-ku, Tokyo, 112-8610, Japan; and* [b] *Experimental Radiology for Children's Health Research Group, National Institute of Radiological Sciences, 4-9-1 Anagawa, Inage-ku, Chiba, 263-8555, Japan*

Miyoshi-Imamura, T., Kakinuma, S., Kaminishi, M., Okamoto, M., Takabatake, T., Nishimura, Y., Imaoka, T., Nishimura, M., Murakami-Murofushi, K. and Shimada, Y. Unique Characteristics of Radiation-Induced Apoptosis in the Postnatally Developing Small Intestine and Colon of Mice. *Radiat. Res.* 173, 310–318 (2010).

We examined the response of the developing mouse intestine to X radiation using neonates (1 day postpartum), infants (2 weeks postpartum) and adults (7 weeks postpartum). Irradiated adult small intestinal crypts displayed two waves of apoptosis. The first wave peaked at 3 h and was followed by a broad wave with a peak persisting from 24 to 48 h. p53 was expressed during the first wave but not the second wave. For the infant small intestine, the intensity of the first wave was approximately half that of the adult wave, and for the colon the intensity was even smaller. In neonates, apoptosis was delayed, peaking at 6 h for small intestinal crypts and at 24 h for colonic crypts. Although no apoptosis occurred at 3 h postirradiation in neonates, p53 was present in both the small intestine and colon, owing at least in part to the inability of p53 to increase the level of Noxa, a p53-dependent pro-apoptosis protein, suggesting a discontinuity in the p53-Noxa-caspase pathway in neonates. By contrast, the induction of p21, a pro-survival protein, was greater in neonatal cells than in adult cells. Thus it appears that the developing and adult intestine mount distinct apoptotic responses to radiation.

INTRODUCTION

Fetuses and young children should not be considered simply as small adults but rather as a unique cohort when assessing the health risks of exposure to environmental carcinogens such as ionizing radiation. Members of this cohort appear to be especially vulnerable to radiation because their organs grow more rapidly and are less differentiated than those of adults. Radiation damage to the tissues has been shown to depend on the degree of cell proliferation and the extent of differentiation. A century ago, Bergonie and Tribondeau stated that "tissues appear to be more radiosensitive if their cells have a greater proliferative capacity, divide more rapidly, and are less-well differentiated" (*1*). The cells of the developing cerebral cortex and the developing kidney are highly susceptible to radiation-induced apoptosis—a sensitivity that is lost after differentiation (*2, 3*). Irradiated hematopoietic and mammary stem cells of weanling mice have been shown to be more severely damaged than those of adult mice (*4, 5*). Exposure of infant mice to 1.5 Gy of radiation depresses their levels of hematopoietic stem cells for a long time thereafter (*6*).

Apoptosis is a form of programmed cell death, i.e., a genetically controlled self-destruction process, occurring during developmental tissue morphogenesis and adult tissue homeostasis (*7*). Apoptosis can be induced by exposure to exogenous DNA-damaging agents including ionizing radiation. Intestinal tract organs of wild-type and genetically engineered adult mice have been used extensively as *in vivo* systems to assess the effects of radiation-induced apoptosis (*8*). The properties that have been monitored include dose response, temporal patterns of apoptosis, spatial distribution of susceptible cells in crypts, differential susceptibilities of small intestinal and colonic epithelial cells and of regions within the colon, and p53, p21 and Bcl-2 activities (*9–24*). However, similar studies using the intestines of neonates and infants have not been undertaken. Therefore, in this study we characterized the features of radiation-induced apoptosis in the postnatally developing small intestine and colon of C57BL/6J mice and compared these features to those of identically treated adult mice. We found that the postnatally developing intestine is more resistant to radiation-induced apoptosis than with the adult intestine, which could be ascribed in part to an apparent inability to completely carry out the post-p53-mediated pathway to apoptosis.

[1] Address for correspondence: Experimental Radiology for Children's Health Research Group, National Institute of Radiological Sciences, 4-9-1 Anagawa, Inage-ku, Chiba, 263-8555, Japan: e-mail: y_shimad@nirs.go.jp.

MATERIALS AND METHODS

Mice

Female C57BL/6J mice were purchased from Charles River Laboratories (Kanagawa, Japan). All mice were exposed to a 12-h dark-light cycle, a temperature of 23 ± 2°C, and 50 ± 10% humidity. They were fed a standard laboratory diet (MB-1; Funabashi Farm Co., Ltd., Chiba, Japan) and given water *ad libitum*. The experimental protocol was reviewed and approved by our institution's animal use committee.

Irradiation of Mice

Irradiation was performed using a Pantak X-ray generator (Pantak Ltd., East Haven, CT). One-day-old (neonate), 2-week-old (infant), and 7-week-old (adult) mice were whole-body irradiated with 2 Gy at a dose rate of 0.7 Gy/min (200 kVp, 20 mA, with a filter composed of 0.5-mm-thick copper and aluminum plates). Subsequently, mice were killed humanely at 0 (unirradiated), 3, 6, 12, 24, 48 and 72 h after irradiation.

Pathology

Unirradiated and irradiated mice were killed after ether anesthesia. Then their small intestines and colons were removed, rinsed in ice-cold phosphate-buffered saline, and fixed quickly in 10% neutral-buffered formalin for about 12 h. Each organ was divided into proximal, middle and distal sections. All samples were embedded in paraffin, sectioned transversely (3–4 μm thick), and stained with hematoxylin and eosin.

Immunohistochemistry

Immunostaining of paraffin-embedded samples followed standard procedures. To retrieve antigens using the primary antibodies [rabbit polyclonal anti-active caspase-3 (1:750, AF835; R&D Systems, Abingdon, UK); rabbit polyclonal anti-p53 (1:500, NCL-p53-CM5; Novocastral Laboratories Ltd., Newcastle, UK); rabbit polyclonal anti-Noxa (1:100, LS-B184/6830; LifeSpan Biosciences, Seattle, WA); rabbit polyclonal anti-p21 (1:500, sc397; Santa Cruz Biotechnology Inc., Santa Cruz, CA); and rat polyclonal anti-Ki-67 (1:100, M7249; DAKO Carpinteria, CA)], the tissue sections in 10 m*M* sodium citrate, pH 6.0, were heated at 120°C for 20 min. After the primary antibodies were washed away, sections were incubated with a peroxidase-conjugated secondary antibody [Histofine® Simple Stain MAX PO(R) or Histofine® Simple Stain MAX PO(Rat); Nichirei Biosciences, Tokyo, Japan]. Peroxidase activity was visualized by first staining with 3,3′-diaminobenzidine (Simple Stain DAB Solution, Nichirei Biosciences, Tokyo, Japan) and then counterstaining with hematoxylin.

Scoring the Numbers and Types of Small Intestinal and Colonic Crypts

The crypt number was defined as the total number of crypts per circumference and was determined by counting the number from crypts found in two to three transverse sections of three mice. For the purpose of identifying the small intestinal crypts, the presence of Paneth cells defined the crypts of mature mice, and clear epithelial invaginations into the mucosa defined the crypts of neonatal and infant mice. We counted a crypt undergoing cleavage, i.e., "crypt fission" or "branching", as two crypts.

Morphologically, apoptosis was defined as the presence of an apoptotic body. This definition correlated well with one that relied on immunohistochemical staining of active caspase 3 (*17*). To quantify the extent of apoptosis, we used two different scoring systems: scoring the number of crypts (as a percentage) containing one or more active caspase 3-positive cells per circumference, and scoring the mean number of apoptotic cells per crypt. However, the extent of apoptosis in the small intestine of 1-day-old mice was scored as the mean number of active caspase 3-positive cells per circumference in the transverse sections, because crypts had not yet formed. The same scoring systems were used to quantify the number of p53-positive crypts (as a percentage) and the mean number of p53-positive cells per crypt. All scoring was performed without knowing whether the mice had been irradiated.

Statistical Analysis

Data are expressed as means ± SEM. Each experiment used three mice. The Student's t test ($P < 0.05$) was used to determine whether experimental values differed significantly between two groups.

RESULTS

Normal Development of Crypts in the Small Intestine and Colon

We first examined the development of intestinal crypts, focusing on morphology and the number of crypts. Plots of the number of crypts present as a function of time and examples of crypt cells expressing Ki-67, reflecting active phases of the cell cycle, are shown in Fig. 1. Supplementary Fig. S1 shows micrographs that document the developmental changes occurring in the anatomical structures of normal small intestinal and colonic crypts between 1 day and 7 weeks postpartum.

1. Small intestine

In the small intestine at 1 day postpartum, invaginating clusters of epithelial cells could be found, but crypts had not yet formed. Morphologically apparent crypts were identified in the proximal region between 4 days and 1 week postpartum and were found next in the middle region and finally in the distal region (Fig. 1A). Then the size and number of crypts increased rapidly (with occasional crypt fission) until 4 weeks postpartum when morphologically mature crypts appeared (Fig. 1A and Supplementary Fig. S1). The number of crypts was nearly constant thereafter (Fig. 1A). Goblet cells were observed 1 day postpartum in the distal region, and Paneth cells, located at the bottom of crypts, developed 1 to 2 weeks postpartum (Supplementary Fig. S1).

At 1 day postpartum, Ki-67 expression was observed in the nuclei of clustered epithelial cells, presumably indicating crypt formation. At 2 weeks postpartum, Ki-67 staining was uniform within a crypt, i.e., was independent of cell position. By 7 weeks postpartum, cells in the proliferative zone (above cell position 4) were most heavily stained (Fig. 1C), as has been reported previously (*18, 19*).

2. Colon

Crypt-like structures were observed at 1 day postpartum (Fig. 1B and Supplementary Fig. S1). Crypt

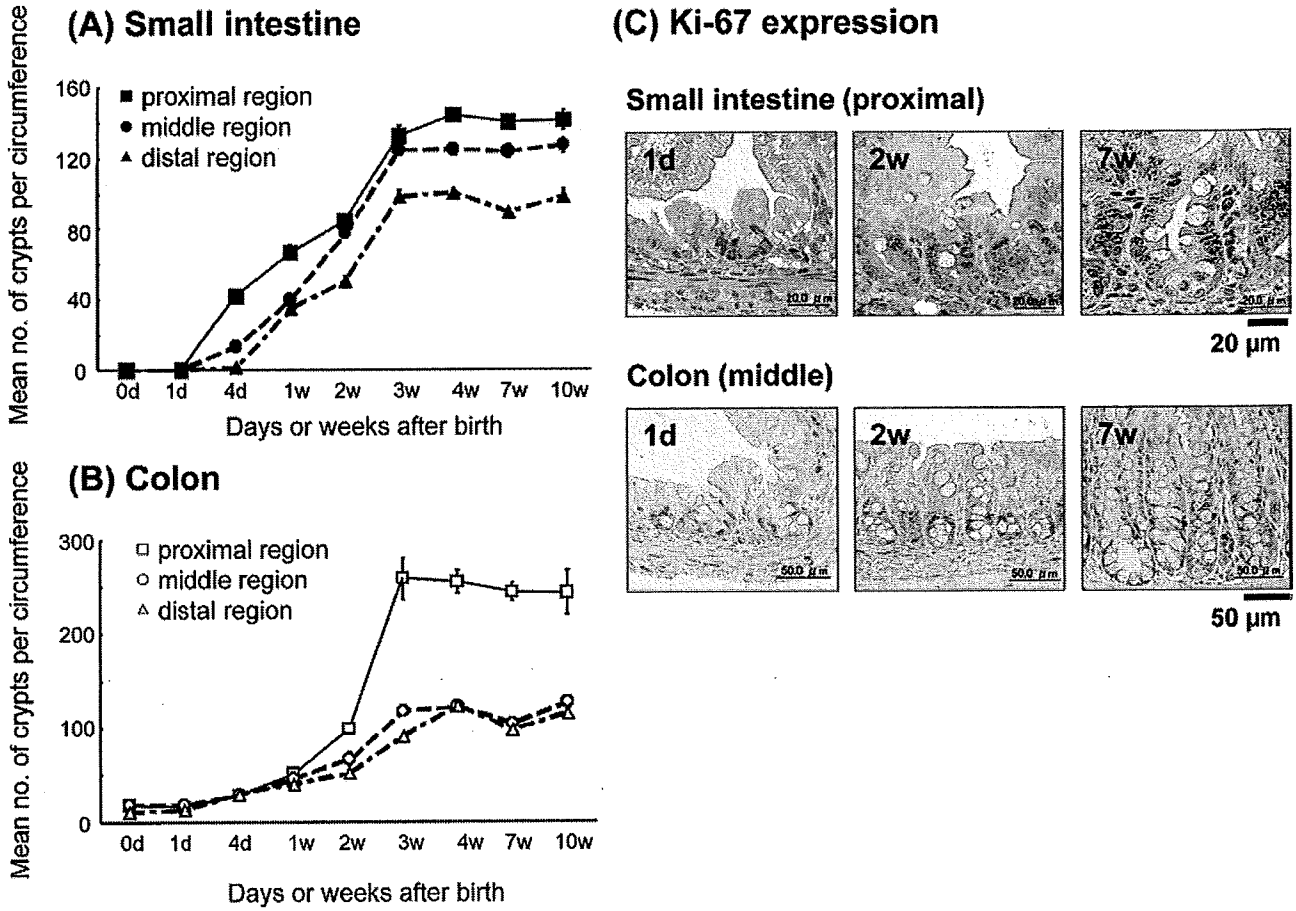

FIG. 1. Developmental changes in the mean number of crypts per circumference for the proximal, middle and distal regions of the small intestine (panel A) and the colon (panel B). Data are reported as means ± SEM. Each experiment used three mice. Panel C: Photomicrographs of Ki-67-stained sections of the small intestine and colon of 1-day-old (1d), 2-week-old (2w) and 7-week-old (7w) mice.

number and size increased with age until 3 to 4 weeks postpartum and were accompanied by frequent crypt fission. Morphologically mature crypts appeared 4 weeks postpartum. The proximal region contained approximately twice as many crypts as did the middle and distal regions (Fig. 1B). Goblet cells developed during the fetal stage (data not shown), which was much earlier than in the small intestine (Supplementary Fig. S1). Ki-67-positive cells were located in the basal one-half to two-thirds of the crypt regardless of age, which was distinctly different from what was seen in the small intestine (Fig. 1C).

Radiation-Induced Apoptosis in Small Intestinal and Colonic Crypts

We next analyzed radiation-induced apoptosis in mice exposed to 2 Gy at 1 day, 2 weeks and 7 weeks postpartum as representatives of neonates with immature or undifferentiated crypts, infants with active proliferative crypts, and adults with a steady number of crypts maintained, respectively (Fig. 1). The dose of 2 Gy was selected based on evidence that the apoptosis in response to ionizing radiation saturates at 1 Gy (*25*). Apoptotic cells were defined as those containing apoptotic bodies and strongly staining for active caspase 3 (*17*). The age and region dependences of the apoptotic response in these mice are shown in Figs. 2, 3 and 4.

1. Small intestine

For mice irradiated at 7 weeks postpartum, apoptosis of crypt cells occurred in two waves (Figs. 2A and 3A). The first wave peaked 3 h after irradiation, as reported previously (*17*), followed by a rapid decrease. The percentage of apoptotic crypts in the first wave was greater than 75% in all regions of the small intestine (Figs. 2A and 4A), and the average number of apoptotic cells was two per crypt (Fig. 3A). The second wave arose thereafter, and its peak level persisted until 48 h. From 10% to 20% of the crypts exhibited apoptosis (Fig. 2A). There were no clear differences among the temporal patterns of the proximal, middle and distal regions (Figs. 2A and 3A). The second apoptotic wave might

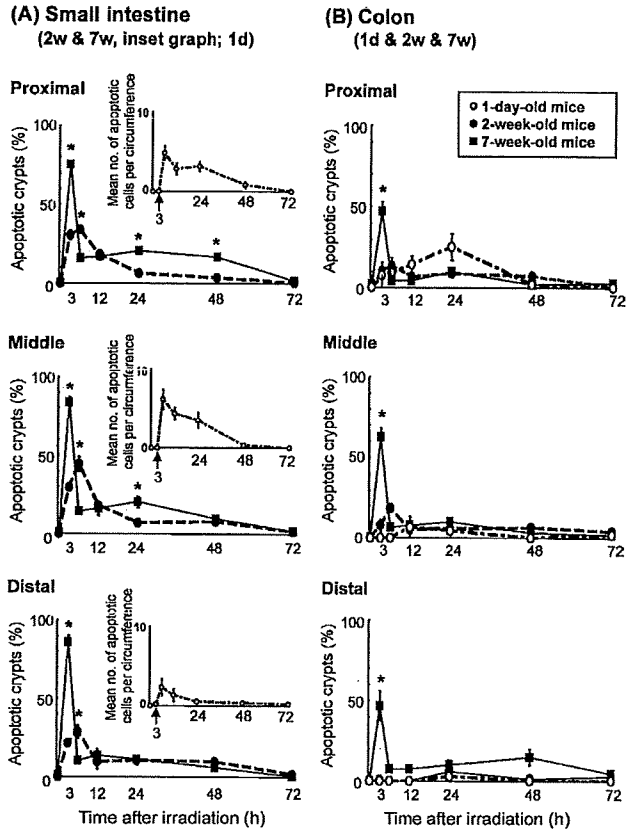

FIG. 2. Percentage of apoptotic crypts as a function of time for the proximal, middle and distal regions of the small intestine (panel A) and the colon (panel B) of mice irradiated at 1 day (1d), 2 weeks (2w) and 7 weeks (7w) postpartum. The inset is a plot of the mean number of apoptotic cells per circumference for 1-day-old irradiated mice. All data are reported as means ± SEM. Each experiment used three mice. For the data points for 2- and 7-week-old mice labeled with an asterisk (*), $P < 0.05$.

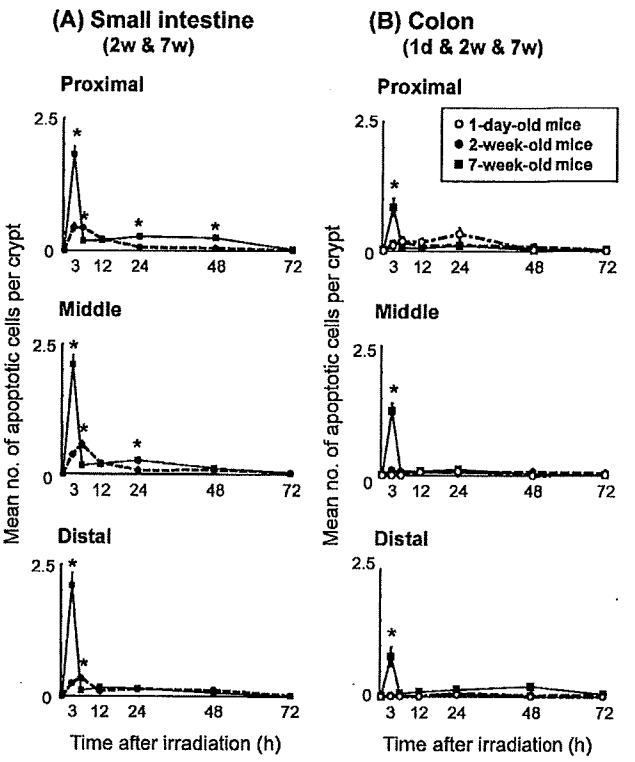

FIG. 3. Mean number of apoptotic cells per crypt as a function of time for the proximal, middle and distal regions of the small intestine of mice irradiated 2 weeks (2w) and 7 weeks (7w) postpartum (panel A) and the colon of mice irradiated 1 day (1d), 2 weeks (2w), and 7 weeks (7w) postpartum (panel B). All data are reported as means ± SEM. Each experiment used three mice. For the data points for 2- and 7-week-old mice labeled with an asterisk (*), $P < 0.05$.

have been the result of a delayed mitotic crisis involving cells that escaped apoptosis during the first wave but then reached the G_2/M checkpoint (*12*).

Compared with the results for 7-week-old mice, the percentage of apoptotic small intestinal crypts in 2-week-old mice at 3 h postirradiation was significantly lower (approximately 20% to 30%; $P < 0.05$; Figs. 2A and 4A). The peak of the first wave occurred 6 h postirradiation, and the average numbers of apoptotic cells per crypt were 0.4, 0.6 and 0.3 for the proximal, middle and distal regions, respectively (Fig. 3A). Only the crypts of the distal region were involved in the second wave of apoptosis (Fig. 2A).

Because no small intestinal crypts were found before the first postpartum day, for the tissues of 1-day-old mice, we used the mean number of apoptotic cells per circumference as a measure of apoptosis. We did not observe any apoptotic cells 3 h after irradiation, instead finding that the maximum apoptosis index occurred at 6 h and persisted until 24 h (Figs. 2A inset and 4A). The mean numbers of apoptotic cells per circumference at 6 h postirradiation were 4.8, 6.2 and 2.3 for the proximal, middle and distal regions, respectively (Fig. 2A insets). At 1 day postpartum, there were approximately 300 to 400 epithelial cells per circumference, which means that approximately 1% of the epithelial cells were very radiosensitive.

2. *Colon*

For 7-week-old mice, the apoptotic response peaked sharply 3 h postirradiation and was followed by a smaller broad response between 24 and 48 h (Figs. 2B, 3B and 4B). Fewer apoptotic cells were found in colonic crypts than in small intestinal crypts (Fig. 3B), as reported previously (*20*). The percentage of apoptotic crypts for the first wave ranged from 47% to 63%, and the average was slightly more than 0.8 apoptotic cell per crypt (Fig. 2B). Conversely, the apoptosis index of colonic crypts of mice irradiated 2 weeks postpartum was much lower, and the maximum values observed for crypts in the proximal and middle regions occurred at 6 h (Fig. 2B). No apoptotic cells were found in the distal region until 12 h postirradiation (Fig. 2B). Colonic cells

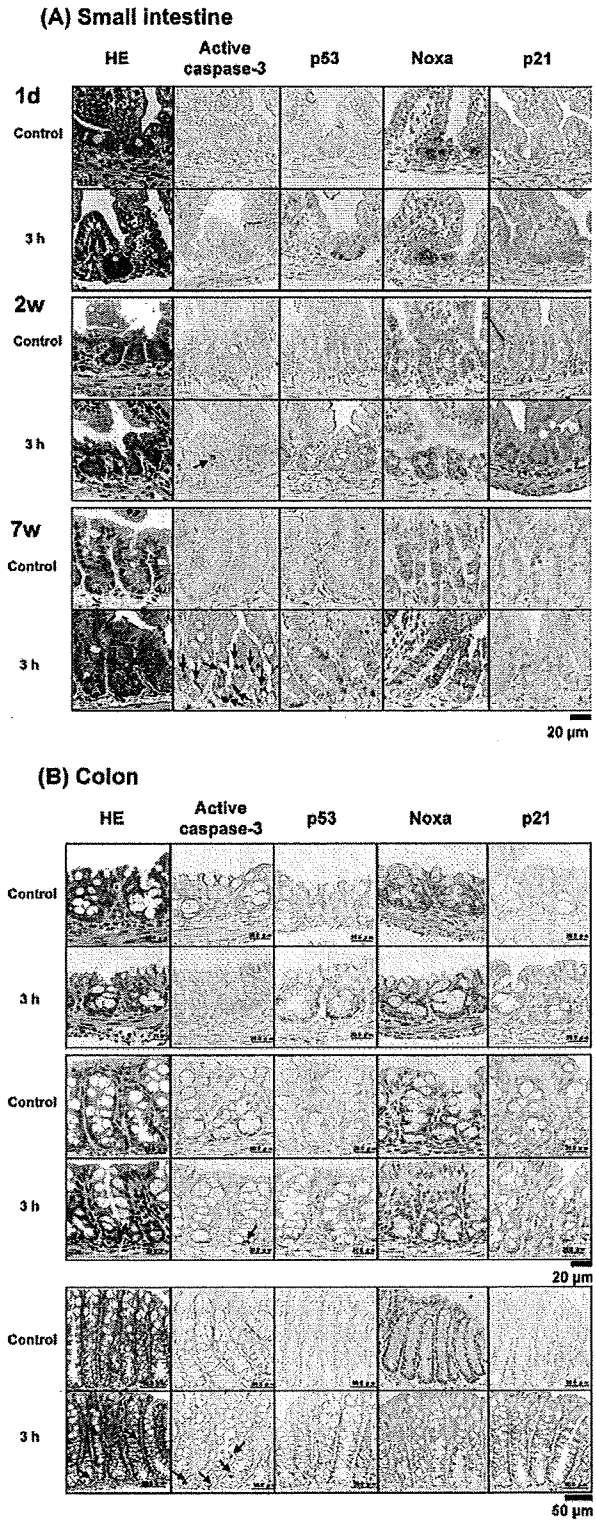

FIG. 4. Photomicrographs of small intestinal (panel A) and colonic (panel B) tissue sections for unirradiated mice and for 1-day-old (1d), 2-week-old (2w) and 7-week-old (7w) mice 3 h after irradiation. From left to right, sections were stained with hematoxylin and eosin or were immunohistologically stained for active caspase 3, p53, Noxa and p21. The arrows point to apoptotic bodies or active caspase 3-positive apoptotic cells.

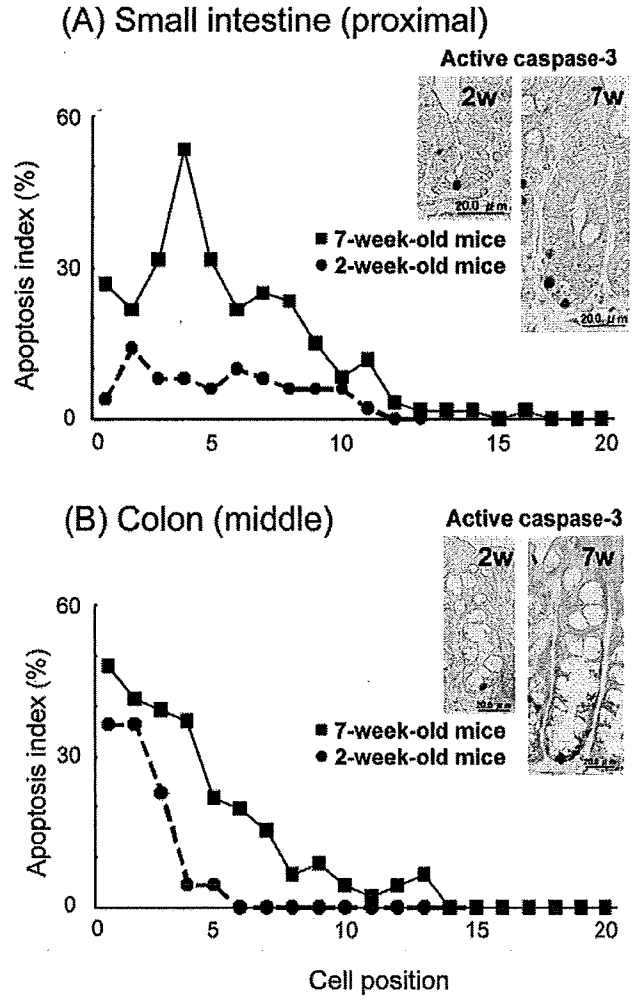

FIG. 5. Age-dependent distribution of apoptotic cells in small intestinal (panel A) and colonic (panel B) crypts. The 2-week-old and 7-week-old mice were irradiated 3 h before being killed. The apoptosis index was calculated using active caspase 3 expression.

irradiated at 1 day postpartum had a unique response to radiation—apoptosis occurred 12 to 24 h postirradiation (Fig. 2B). Moreover, there were regional differences in the mean numbers of apoptotic cells present. The maximum apoptosis index was greater for the proximal colon than for the middle region, and few if any apoptotic crypts were seen in the distal region during the 72-h postirradiation period (Figs. 2B and 3B).

Distribution of Apoptotic Cells in the Small Intestine and Colon

The distribution of apoptotic cells along small intestinal and colonic crypt lengths was determined for 22–50 apoptotic half-crypts of irradiated mice at 2 and 7 weeks of age. The distribution at 3 h postirradiation is shown in Fig. 5. Small intestinal crypts in 7-week-old irradiated mice showed a characteristic peak in the

apoptosis index around cell position 4, a putative stem cell site (*17, 20, 21*). In this study, the small intestinal crypts of 2-week-old mice had smaller apoptosis indices than did those of the adult intestine. Additionally, no specific cell position was associated with a greater radiosensitivity than was any other; instead, similar values for the apoptosis index were broadly distributed as the base of the crypt was approached. Conversely, the frequency of apoptosis in colonic crypts of 7-week-old mice was greatest at cell positions 1–4, the putative stem cell zone (*17, 20*), and declined as the cell position number increased. The colons of 2-week-old mice also had apoptotic cells at the bottom of crypts. These results suggest that normal differentiation of small intestinal cells leads to susceptibility to radiation-induced apoptosis uniquely at cell position 4 during development of the crypt functional architecture, whereas colon cells remain unchanged with regard to cell position-associated radiosensitivity, as indicated by the lack of a difference between 2- and 7-week-old mice.

p53, Noxa and p21 Expression

We examined the age dependence of expression of p53, Noxa and p21, each of which is a crucial determinant of apoptosis (Figs. 4 and 6). Expression of p53 was observed 3 h postirradiation in the cells of the basal half of most intestinal crypts of 7-week-old mice (Fig. 4A and B). Eighty-one percent of the small intestinal crypts were p53 positive, and 100% of the colonic crypts were p53 positive (Fig. 6). Expression of p53 was also high in small intestinal and colonic crypts of irradiated 2-week-old mice, with frequencies of 86% and 95%, respectively. Notably, the apoptosis indices of 2-week-old mice were much lower than those of 7-week-old mice for both the small intestinal and colonic crypts (Fig. 6). Significant p53 expression also occurred in the intestinal crypts of irradiated 1-day-old mice (Fig. 6). Small intestinal cells expressing p53 were clustered in the intervillus region (Fig. 4A); those of the colon were restricted to cells in newly forming crypts (Fig. 4B). It is possible that a link between p53 expression and apoptosis does not exist in the intestine of 1-day- and 2-week-old mice. The levels of p53 expression in the intestinal crypts of 1-day-, 2-week- and 7-week-old mice were negligible at 24 h postirradiation (during the second wave of apoptosis), suggesting that apoptosis was independent of p53 during this time (Fig. 6).

To further characterize the apoptotic response, we immunohistochemically examined the expression of the p53-dependent pro-death factor, Noxa, and pro-survival factor, p21, in the intestinal epithelia of 1-day-old, 2-week-old and 7-week-old irradiated mice. In the small intestine of irradiated 7-week-old mice, Noxa expression increased markedly in cells at positions greater than 4 compared to unirradiated cells, and the expression was

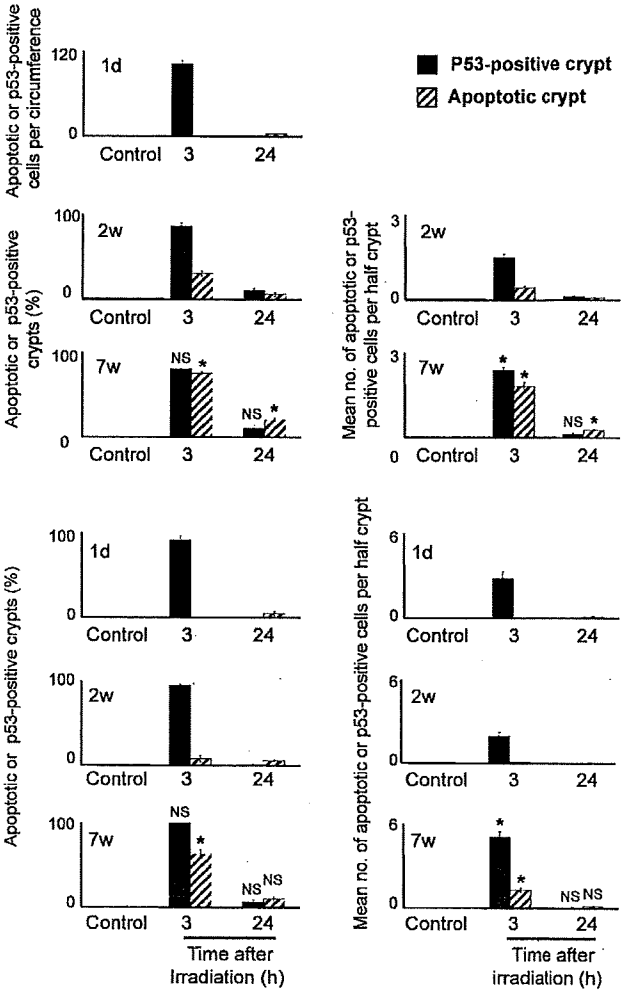

FIG. 6. Percentages of apoptotic crypts and p53-positive crypts (left column) and the mean numbers of apoptotic and p53-positive cells per half crypt (right column) present in tissue sections of the proximal small intestine (panel A) and the colon (panel B) of irradiated mice. For the data for small intestine tissue presented in the right column, mice were 2 weeks old (2w) or 7 weeks old (7w). For 1-day-old (1d) mice, the data for small intestine tissue in the right column are presented as the mean number of apoptotic or p53-positive cells per circumference. Times were 3 h and 24 h after irradiation. The control group was not irradiated. Data are reported as means ± SEM. Each experiment used three mice. For the data points for 7-week-old mice labeled with an asterisk (*), $P < 0.05$ compared to 2-week-old mice.

clearly visible (see dots in Fig. 4A). In irradiated 2-week-old mice, this expression was moderately induced compared to that in 7-week-old mice (Fig. 4A). Unexpectedly, the intervillus region of the small intestine of 1-day-old neonates expressed a substantial amount of Noxa, but the expression level was not influenced by radiation (Fig. 4A). In the colon, Noxa expression was less than that in the small intestine at all ages examined, which may correlate with the relatively low frequency of apoptosis compared to the small intestine (Fig. 4B). The

level of Noxa expression after irradiation in the colonic epithelial cells of 7-week-old mice was increased only slightly. By contrast, in 1-day-old and 2-week-old mice, Noxa expression remained almost unchanged after irradiation (Fig. 4B).

The basal p21 expression levels in the nuclei of small intestinal crypts were the same for 7-week-old mice regardless of whether they had been irradiated. The level of p21 expression increased slightly in cells of 2-week-old irradiated mice. At 1 day postpartum, strong p21 expression was observed both in the nuclei of clustered cells and the cytoplasm of villus and intervillus epithelial cells (Fig. 4A). For the colonic cells of all mice examined, p21 expression was always greater when the mice had been irradiated, as reported previously (*22*). The expression of p21 occurred in the nuclei of cells within the proliferative zone in adult crypts of 7-week-old mice, whereas it occurred throughout crypts of 1-day- and 2-week-old mice (Fig. 4B).

DISCUSSION

For this study, we documented the developmental changes that occur in the small intestine and colon of mice in response to ionizing radiation, an inducer of apoptosis. Unexpectedly, the rapidly growing intestinal epithelial cells of neonatal and infant mice were more radioresistant than were those of adults. Three notable differences were found for how adult and immature crypt cells responded to radiation, as follows. Immature epithelial cells had a delayed first wave of apoptosis in comparison with those of adults. Cells that were extraordinarily susceptible to radiation at mature crypt position 4 were not absorbed in the immature crypt. Especially in neonates, regional differences in radiosensitivities along the intestinal tract were also found—the cells of the small intestinal and colonic distal regions were more radioresistant than were those of the proximal regions.

It has been believed that actively proliferating, immature, undifferentiated epithelial cells are much more sensitive to radiation-induced apoptosis than are differentiated cells (*2–5, 26*). However, as we report here, the intestinal epithelial cells of neonatal and infant mice were more resistant to radiation-induced apoptosis than were those of adults. It has been reported that a dynamic balance between pro-survival and pro-death proteins may determine whether cells undergo apoptosis (*27–29*). In this study, p53 accumulated in irradiated cells regardless of the age of the mouse, whereas there were marked differences in the expression levels of Noxa (a p53-induced pro-apoptosis protein) and p21 (a pro-survival protein) between neonatal, infant and adult intestines. Noxa expression in irradiated adult small intestine increased markedly over the basal level, whereas this was not the case in irradiated neonatal mice. By contrast, p21 expression increased significantly in the cytoplasm and nucleus of neonatal cells in comparison with adult cells. It has been reported that nuclear p21 is necessary for cell cycle arrest (*30, 31*), whereas cytoplasmic p21 inhibits an initiator caspase (*32, 33*). Therefore, after radiation-induced DNA damage, p53 may only marginally induce the expression of pro-apoptosis proteins in neonatal intestinal cells, whereas the cell cycle of neonatal intestinal cells may be arrested efficiently by p53, allowing the cell time to repair its DNA and prevent apoptosis. The balance between cell cycle arrest and apoptosis in response to DNA damage probably changes with development.

Another possible mechanism underlying the radioresistance of neonatal and infant epithelial cells is related to the increased expression of cellular Bcl-2. Bcl-2, which is survival factor, is expressed throughout the intestinal epithelium at embryonic day 14.5 (*34*). At embryonic day 18.5, Bcl-2 expression is restricted to the base of villi; in adult cells, it has been detected in only a small fraction of crypt cells (*11*). Thus the different radiosensitivities of the adult and infant small intestine and colon may be partly explained by their distinctly different Bcl-2 expression profiles (*11, 13, 14*). It was recently found that Wnt/beta-catenin mediates the radioresistance of mouse mammary progenitor cells (*35*). The Wnt signaling pathway is intimately involved in the regulation of intestinal development and maintenance (*36–40*). During the late fetal period, Wnt signaling occurs in newly formed villi and by 3 days postpartum in intervillus cells. After weaning, Wnt activity is confined to the cells of the crypt base (*41*). Therefore, developmental changes in Bcl-2 activity and Wnt signaling may also account in part for radioresistance. Additionally, radioresistance may also be associated with the degree to which cells can repair DNA damage, the rate and mode of stem cell division, and the type and abundance of intestinal microflora present (*42–45*).

Potten has hypothesized that the observed greater resistance to apoptosis by colonic crypts (compared with small intestinal crypts) may account for the greater incidence of colonic carcinoma (*24, 46*). We found here that neonatal and infant intestinal epithelial cells were more resistant to radiation-induced apoptosis than were those of adults. Temporally, $Apc^{Min/+}$ mice, a murine model of human familial adenomatous polyposis, have been shown to be most sensitive to intestinal tumor induction when irradiated at 10 to 12 days of age (*47, 48*). This age-related tumor susceptibility could be explained by a failure of cells with sustained DNA damage to undergo apoptosis and is a possible mechanism carcinogenesis that is consistent with Potten's proposal (*24, 46*).

In conclusion, we demonstrated that, in the developing intestine of C57BL/6J mice, the extent of radiation-induced apoptosis is dependent on age, tissue type and

organ region. Neonatal and infant intestinal epithelial cells were more resistant to radiation-induced apoptosis than were those of adults. When the molecular mechanisms underlying age-related radiosensitivity are better characterized, it may be possible to predict more accurately when children exposed to radiation will develop cancer and use preventive measures to decrease their risk.

SUPPLEMENTARY INFORMATION

Supplementary Fig. S1. Photomicrographs of transverse sections of small intestinal (A) and colonic (B) tissue taken from unirradiated female mice between the ages of 1 day (1d) and 7 weeks postpartum (7w). The arrows labeled A point to clusters of epithelial cells. Arrows labeled B point to crypts undergoing fission. http://dx.doi.org/10.1667/RR1905.1.S1

ACKNOWLEDGMENTS

We thank Drs. K. Yamauchi, Y. Morita, H. Kawame, Y. Kakiuchi and K. Takizawa for helpful comments. We are also greatly thankful to Ms. E. Obara and Y. Amasaki for their technical and secretarial assistance, and to all members of the Division of Animal Facility for help with animal maintenance. This study was financially supported in part by Grants-in-Aid for Scientific Research from the Ministry of Education, Culture, Sports, Science, and Technology, Grants-in-Aid for Cancer Research and Third-Term Comprehensive Strategy for Cancer Control from the Ministry of Health, Labour and Welfare, and a grant from the Long-range Research Initiative (LRI) of the Japan Chemical Industry Association (JCIA).

Received: June 23, 2009; accepted: October 14, 2009; published online: December 8, 2009

REFERENCES

1. J. Bergonie and L. Tribondeau, Interpretation of some results from radiotherapy and an attempt to determine a rational treatment technique. 1906. *Yale J. Biol. Med.* **76**, 181–182 (2003). [originally published in *C. R. Seances Acad. Sci.* **143**, 983–985 (1906)]
2. I. Ferrer, The effect of cycloheximide on natural and X-ray-induced cell death in the developing cerebral cortex. *Brain Res.* **588**, 351–357 (1992).
3. G. C. Gobe, R. A. Axelsen, B. V. Harmon and D. J. Allan, Cell death by apoptosis following X-irradiation of the foetal and neonatal rat kidney. *Int. J. Radiat. Biol.* **54**, 567–576 (1988).
4. S. S. Fred and W. W. Smith, Radiation sensitivity and proliferative recovery of hemopoietic stem cells in weanling as compared to adult mice. *Radiat. Res.* **32**, 314–326 (1967).
5. Y. Shimada, J. Yasukawa-Barnes, R. Y. Kim, M. N. Gould and K. H. Clifton, Age and radiation sensitivity of rat mammary clonogenic cells. *Radiat. Res.* **137**, 118–123 (1994).
6. G. B. Gerber and J. Maes, Stem cell kinetics in spleen and bone marrow after single and fractionated irradiation of infant mice. *Radiat. Environ. Biophys.* **18**, 249–256 (1980).
7. A. G. Renehan, C. Booth and C. S. Potten, What is apoptosis, and why is it important? *Br. Med. J.* **322**, 1536–1538 (2001).
8. A. J. Watson and D. M. Pritchard, Lessons from genetically engineered animal models. VII. Apoptosis in intestinal epithelium: lessons from transgenic and knockout mice. *Am. J. Physiol. Gastrointest. Liver Physiol.* **278**, G1–G5 (2000).
9. A. R. Clarke, S. Gledhill, M. L. Hooper, C. C. Bird and A. H. Wyllie, p53 dependence of early apoptotic and proliferative responses within the mouse intestinal epithelium following gamma-irradiation. *Oncogene* **9**, 1767–1773 (1994).
10. A. J. Merritt, C. S. Potten, C. J. Kemp, J. A. Hickman, A. Balmain, D. P. Lane and P. A. Hall, The role of p53 in spontaneous and radiation-induced apoptosis in the gastrointestinal tract of normal and p53-deficient mice. *Cancer Res.* **54**, 614–617 (1994).
11. A. J. Merritt, C. S. Potten, A. J. Watson, D. Y. Loh, K. Nakayama, K. Nakayama and J. A. Hickman, Differential expression of bcl-2 in intestinal epithelia. Correlation with attenuation of apoptosis in colonic crypts and the incidence of colonic neoplasia. *J. Cell Sci.* **108**, 2261–2271 (1995).
12. A. J. Merritt, T. D. Allen, C. S. Potten and J. A. Hickman, Apoptosis in small intestinal epithelial from p53-null mice: evidence for a delayed, p53-independent G_2/M-associated cell death after gamma-irradiation. *Oncogene* **14**, 2759–2766 (1997).
13. K. P. Hoyes, W. B. Cai, C. S. Potten and J. H. Hendry, Effect of bcl-2 deficiency on the radiation response of clonogenic cells in small and large intestine, bone marrow and testis. *Int. J. Radiat. Biol.* **76**, 1435–1442 (2000).
14. D. M. Pritchard, C. S. Potten, S. J. Korsmeyer, S. Roberts and J. A. Hickman, Damage-induced apoptosis in intestinal epithelia from bcl-2-null and bax-null mice: investigations of the mechanistic determinants of epithelial apoptosis in vivo. *Oncogene* **18**, 7287–7293 (1999).
15. D. M. Pritchard, C. Print, L. O'Reilly, J. M. Adams, C. S. Potten and J. A. Hickman, Bcl-w is an important determinant of damage-induced apoptosis in epithelia of small and large intestine. *Oncogene* **19**, 3955–3959 (2000).
16. K. Martin, C. S. Potten and T. B. Kirkwood, Age-related changes in irradiation-induced apoptosis and expression of p21 and p53 in crypt stem cells of murine intestine. *Ann. NY Acad. Sci.* **908**, 315–318 (2000).
17. E. Marshman, P. D. Ottewell, C. S. Potten and A. J. Watson, Caspase activation during spontaneous and radiation-induced apoptosis in the murine intestine. *J. Pathol.* **195**, 285–292 (2001).
18. W. S. el-Deiry, T. Tokino, T. Waldman, J. D. Oliner, V. E. Velculescu, M. Burrell, D. E. Hill, E. Healy, J. L. Rees and B. Vogelstein, Topological control of p21WAF1/CIP1 expression in normal and neoplastic tissues. *Cancer Res.* **55**, 2910–2919 (1995).
19. C. S. Potten, Stem cells in gastrointestinal epithelium: numbers, characteristics and death. *Phil. Trans. R. Soc. Lond. B Biol. Sci.* **353**, 821–830 (1998).
20. C. S. Potten and H. K. Grant, The relationship between ionizing radiation-induced apoptosis and stem cells in the small and large intestine. *Br. J. Cancer* **78**, 993–1003 (1998).
21. C. S. Potten, Radiation, the ideal cytotoxic agent for studying the cell biology of tissues such as the small intestine. *Radiat. Res.* **161**, 123–136 (2004).
22. J. W. Wilson, D. M. Pritchard, J. A. Hickman and C. S. Potten, Radiation-induced p53 and p21WAF-1/CIP1 expression in the murine intestinal epithelium: apoptosis and cell cycle arrest. *Am. J. Pathol.* **153**, 899–909 (1998).
23. C. S. Potten, C. Booth and D. Hargreaves, The small intestine as a model for evaluating adult tissue stem cell drug targets. *Cell Prolif.* **36**, 115–129 (2003).
24. E. Marshman, C. Booth and C. S. Potten, The intestinal epithelial stem cell. *Bioessays* **24**, 91–98 (2002).
25. C. S. Potten, A. Merritt, J. Hickman, P. Hall and A. Faranda, Characterization of radiation-induced apoptosis in the small intestine and its biological implications. *Int. J. Radiat. Biol.* **65**, 71–78 (1994).
26. I. Szumiel, Ionizing radiation-induced cell death. *Int. J. Radiat. Biol.* **66**, 329–341 (1994).

27. P. Fei, E. J. Bernhard and W. S. El-Deiry, Tissue-specific induction of p53 targets in vivo. *Cancer Res.* **62**, 7316–7327 (2002).
28. S. N. Willis and J. M. Adams, Life in the balance: how BH3-only proteins induce apoptosis. *Curr. Opin. Cell Biol.* **17**, 617–625 (2005).
29. J. Yu and L. Zhang, The transcriptional targets of p53 in apoptosis control. *Biochem. Biophys. Res. Commun.* **331**, 851–858 (2005).
30. F. Goubin and B. Ducommun, Identification of binding domains on the p21Cip1 cyclin-dependent kinase inhibitor. *Oncogene* **10**, 2281–2287 (1995).
31. C. J. Sherr and J. M. Roberts, Inhibitors of mammalian G1 cyclin-dependent kinases. *Genes Dev.* **9**, 1149–1163 (1995).
32. S. Q. Xu and W. S. El-Deiry, p21(WAF1/CIP1) inhibits initiator caspase cleavage by TRAIL death receptor DR4. *Biochem. Biophys. Res. Commun.* **269**, 179–190 (2000).
33. M. Asada, T. Yamada, H. Ichijo, D. Delia, K. Miyazono, K. Fukumuro and S. Mizutani, Apoptosis inhibitory activity of cytoplasmic p21(Cip1/WAF1) in monocytic differentiation. *EMBO J.* **18**, 1223–1234 (1999).
34. D. V. Novack and S. J. Korsmeyer, Bcl-2 protein expression during murine development. *Am. J. Pathol.* **145**, 61–73 (1994).
35. W. A. Woodward, M. S. Chen, F. Behbod, M. P. Alfaro, T. A. Buchholz and J. M. Rosen, WNT/beta-catenin mediates radiation resistance of mouse mammary progenitor cells. *Proc. Natl. Acad. Sci. USA* **104**, 618–623 (2007).
36. D. Pinto, A. Gregorieff, H. Begthel and H. Clevers, Canonical Wnt signals are essential for homeostasis of the intestinal epithelium. *Genes Dev.* **17**, 1709–1713 (2003).
37. J. Hoffman, F. Kuhnert, C. R. Davis and C. J. Kuo, Wnts as essential growth factors for the adult small intestine and colon. *Cell Cycle* **3**, 554–557 (2004).
38. F. Kuhnert, C. R. Davis, H. T. Wang, P. Chu, M. Lee, J. Yuan, R. Nusse and C. J. Kuo, Essential requirement for Wnt signaling in proliferation of adult small intestine and colon revealed by adenoviral expression of Dickkopf-1. *Proc. Natl. Acad. Sci. USA* **101**, 266–271 (2004).
39. M. van de Wetering, E. Sancho, C. Verweij, W. de Lau, I. Oving, A. Hurlstone, K. van der Horn, E. Batlle, D. Coudreuse and H. Clevers, The beta-catenin/TCF-4 complex imposes a crypt progenitor phenotype on colorectal cancer cells. *Cell* **111**, 241–250 (2002).
40. V. Korinek, N. Barker, P. Moerer, E. van Donselaar, G. Huls, P. J. Peters and H. Clevers, Depletion of epithelial stem-cell compartments in the small intestine of mice lacking Tcf-4. *Nat. Genet.* **19**, 379–383 (1998).
41. B. M. Kim, J. Mao, M. M. Taketo and R. A. Shivdasani, Phases of canonical Wnt signaling during the development of mouse intestinal epithelium. *Gastroenterology* **133**, 529–538 (2007).
42. I. L. Steffensen, H. A. Schut, J. E. Paulsen, A. Andreassen and J. Alexander, Intestinal tumorigenesis in multiple intestinal neoplasia mice induced by the food mutagen 2-amino-1-methyl-6-phenylimidazo[4,5-b]pyridine: perinatal susceptibility, regional variation, and correlation with DNA adducts. *Cancer Res.* **61**, 8689–8696 (2001).
43. C. S. Potten, G. Owen and D. Booth, Intestinal stem cells protect their genome by selective segregation of template DNA strands. *J. Cell Sci.* **115**, 2381–2388 (2002).
44. J. L. Sherley, P. B. Stadler and D. R. Johnson, Expression of the wild-type p53 antioncogene induces guanine nucleotide-dependent stem cell division kinetics. *Proc. Natl. Acad. Sci. USA* **92**, 136–140 (1995).
45. J. R. Merok, J. A. Lansita, J. R. Tunstead and J. L. Sherley, Cosegregation of chromosomes containing immortal DNA strands in cells that cycle with asymmetric stem cell kinetics. *Cancer Res.* **62**, 6791–6795 (2002).
46. C. S. Potten, Y. Q. Li, P. J. O'Connor and D. J. Winton, A possible explanation for the differential cancer incidence in the intestine, based on distribution of the cytotoxic effects of carcinogens in the murine large bowel. *Carcinogenesis* **13**, 2305–2312 (1992).
47. M. Okamoto and H. Yonekawa, Intestinal tumorigenesis in Min mice is enhanced by X-irradiation in an age-dependent manner. *J. Radiat. Res. (Tokyo)* **46**, 83–91 (2005).
48. M. Ellender, J. D. Harrison, R. Kozlowski, M. Szluinska, S. D. Bouffler and R. Cox, *In utero* and neonatal sensitivity of $Apc^{Min/+}$ mice to radiation-induced intestinal neoplasia. *Int. J. Radiat. Biol.* **82**, 141–151 (2006).

Mutation Research 686 (2010) 30–38

Contents lists available at ScienceDirect

Mutation Research/Fundamental and Molecular Mechanisms of Mutagenesis

journal homepage: www.elsevier.com/locate/molmut

Community address: www.elsevier.com/locate/mutres

Complicated biallelic inactivation of *Pten* in radiation-induced mouse thymic lymphomas

Yu Yamaguchi[a,b,1,2], Takashi Takabatake[b,1], Shizuko Kakinuma[b], Yoshiko Amasaki[b], Mayumi Nishimura[b], Tatsuhiko Imaoka[b], Kazumi Yamauchi[b], Yi Shang[b], Tomoko Miyoshi-Imamura[b,c], Hiroyuki Nogawa[a], Yoshiro Kobayashi[d], Yoshiya Shimada[b,*]

[a] *Department of Biology, Graduate School of Science, Chiba University, Yayoicho, Inage-ku, Chiba 263-8522, Japan*
[b] *Experimental Radiobiology for Children's Health Research Group, Research Center for Radiation Protection, National Institute of Radiological Sciences, 4-9-1, Anagawa, Inage-ku, Chiba 263-8555, Japan*
[c] *Genetic Counseling Program, Graduate School of Humanities and Sciences, Ochanomizu University, 2-1-1 Otsuka, Bunkyou-ku, Tokyo 112-8610, Japan*
[d] *Department of Biomolecular Science, Faculty of Science, Toho University, Miyama 2-2-1, Funabashi, Chiba 274-8510, Japan*

ARTICLE INFO

Article history:
Received 29 September 2009
Accepted 29 December 2009
Available online 7 January 2010

Keywords:
Pten
Thymic lymphoma
Epigenetic silencing
Mutation
Deletion
Radiation

ABSTRACT

Inactivation of the phosphatase and tensin homolog gene (*Pten*) occurs via multiple tissue-dependent mechanisms including epigenetic silencing, point mutations, insertions, and deletions. Although frequent loss of heterozygosity around the *Pten* locus and plausible involvement of epigenetic silencing have been reported in radiation-induced thymic lymphomas, the proportion of lymphomas with inactivated *Pten* and the spectrum of causal aberrations have not been extensively characterized. Here, we assessed the mode of *Pten* inactivation by comprehensive analysis of the expression and alteration of *Pten* in 23 radiation-induced thymic lymphomas developed in B6C3F1 mice. We found no evidence for methylation-associated silencing of *Pten*; rather, complex structural abnormalities comprised of missense and nonsense mutations, 1- and 3-bp insertions, and focal deletions were identified in 8 of 23 lymphomas (35%). Sequencing of deletion breakpoints suggested that aberrant V(D)J recombination and microhomology-mediated rearrangement were responsible for the focal deletions. Seven of the 8 lymphomas had biallelic alterations, and 4 of them did not express Pten protein. These *Pten* aberrations coincided with downstream Akt phosphorylation. In conclusion, we demonstrate that *Pten* inactivation is frequently biallelic and is caused by a variety of structural abnormalities (rather than by epigenetic silencing) and is involved in radiation-induced lymphomagenesis.

1. Introduction

The phosphatase and tensin homolog (Pten) is an important lipid phosphatase that antagonizes the phosphatidylinositol-3-kinase (PI3K)/Akt signaling pathway [1,2]. The PI3K/Akt signaling pathway is aberrantly activated in a variety of tumors, often resulting from defects in the *PTEN* gene [3,4]. Once activated, Akt promotes fundamental cellular processes such as cell survival, growth, proliferation, angiogenesis, and cellular metabolism. Pten also plays a crucial role as guardian of genome integrity by maintaining chromosomal stability through physical interaction with centromeres and by controlling DNA repair, both of which are independent of Akt activation [5].

PTEN is mutated in a variety of human carcinomas [6,7], and *PTEN* is the second most frequently mutated gene in human cancers after *TP53* [8,9]. Germline mutations of *PTEN* in humans are responsible for Cowden disease, which is characterized by a high risk for thyroid and breast cancers [10]. In addition to genetic alterations resulting in missense, nonsense or frameshift mutations, epigenetic silencing of *PTEN* has been reported in the pathogenesis of gastric and breast cancers [11,12]. Furthermore, overexpression of *PTEN*-targeting microRNAs correlates with decreased expression of PTEN protein in hepatocellular [13] and ovarian cancers [14]. These reports indicate that there are multiple mechanisms responsible for *PTEN* inactivation.

Interestingly, there are significant differences in the location of mutations in *PTEN* with respect to cancer type. For example, a high proportion of glioblastomas have missense mutations in exon 6, which encodes part of the phosphatase domain of PTEN, whereas few mutations have been found in exons 7 and 8, which encode

* Corresponding author. Tel.: +81 43 206 3200; fax: +81 43 206 4138.
E-mail address: y_shimad@nirsgo.jp (Y. Shimada).
[1] These authors contributed equally to this study.
[2] Present address: Pharmaceutical Research Laboratories, Sanwa Kagaku, Kenkyusho Co., Ltd., 363 Shiosaki, Hokusei-cho, Inabe-shi, Mie 511-0406, Japan.

0027-5107/$ – see front matter © 2010 Elsevier B.V. All rights reserved.
doi:10.1016/j.mrfmmm.2009.12.011

Table 1
Summary of expression and aberrations of Pten in 23 thymic lymphomas, in parallel with the activation of a downstream factor of Akt.

Tumor ID	LOH[a] status	Structural alteretations[b]	Transcriptional changes[b]	Predicted changes[c]	Pten protein	Akt protein[d]
TL5	–	Duplication of exon6 and exon7 509 Ins TGT	Additional faint long product nd	Ins of 103 amino acids 170S → M and C	A faint larger band Low	Activated
TL14	C3H	Del of exon4 and exon5 9621ns A	Additional faint short product nd	Stop at codon264 Stop at codon333	Absent Absent	Activated
TL8	B6	Homozygous deletion	Absent	–	Absent	Activated
TL11	C3H	Homozygous deletion	Aberant splicing	Stop at codon54	Absent	Activated
TL20	B6	Homozygous deletion	Lack of sequence for exon 1	–	Absent	Activated
TL15	–	862 G → G/T	nd	Stop codon	Low	Activated
TL19	C3H	158 T → T/C[e]	nd	53 V → A	Low	nd
TL21	C3H	364 A → T	nd	122 I → F	Low	Activated
TL12	C3H	nd	nd	–	Low	Activated
TL3	–	nd	nd	–	Low	nd
TL6	–	nd	nd	–	Low	nd

[a] Lost allele is shown. (–), retention of heterozygosity.
[b] Ins, insertion; Del, deletion; nd, not detected.
[c] S, serine; M, methionine; C, cysteine; V, valine; A, alanine; I, isoleucine; F, phenylalanine.
[d] "Activated" means that the phosphorylation of Akt protein at Ser473 was detected; nd, not detected.
[e] Sequencing analysis indicates the presence of both mutated and non-mutated sequence, the latter of which may be due to contaminated normal cells.

the C2 domain. In contrast, endometrial carcinomas rarely contain mutations in exon 6; rather, frameshift mutations in exons 7 and 8 are common [6,7]. Deletion of *PTEN* has been identified in 77% of prostate cancer cases, with 25% containing homozygous deletions [15]. Because previous studies have examined only single or limited categories of causal alterations, the overall contribution of each causal *PTEN* alteration remains unclear for many tumor types.

Radiation is a clear etiology for leukemia and lymphoma. Radiation-induced murine thymic lymphomas have been used as a suitable model of human T-cell acute lymphoblastic leukemia (ALL), many of which exhibit *Notch1* and *Ikaros* mutation, *p15* and *p16* alteration, and aberrant activation of Jak-Stat signaling [16–20]. Loss of heterozygosity (LOH) within a broad genomic region of chromosome 19, including the mouse *Pten* locus, has been demonstrated in many thymic lymphomas [21,22]. Although it has been suggested that *Pten* undergoes epigenetic silencing by DNA methylation in radiation-induced murine thymic lymphomas [22], direct evidence has not yet been reported.

To identify the mode of *Pten* inactivation in hematopoietic malignancies, we systematically analyzed the status of *Pten* alleles and Pten expression at the RNA and protein levels in 23 radiation-induced thymic lymphomas developed in B6C3F1 mice; downstream activation of Akt was also analyzed. These analyses revealed that biallelic structural abnormality of *Pten*, but not epigenetic silencing, plays a significant role in radiation-induced lymphomagenesis.

2. Materials and methods

2.1. Tumor induction

The induction of thymic lymphomas was carried out as described [23], with minor modifications. In brief, female B6C3F1 mice were exposed weekly to 2.0 Gy whole-body X-ray radiation for four consecutive weeks starting at four weeks of age. Mice were observed daily until moribund and were then sacrificed under ether anesthesia. All experiments with mice were conducted according to the legal regulations in Japan and were in compliance with the guidelines for the care of laboratory animals of the National Institute of Radiological Sciences.

2.2. LOH analysis

For LOH analysis, genomic DNA was amplified by PCR using the following polymorphic markers: *D19Mit59*, *D19Mit46*, *D19Mit19*, *D19Mit53* and *D19Mit34* (see Supplementary Table 1). To determine LOH at the *Pten* locus, the microsatellite sequence was searched using the UCSC Genome Bioinformatics database (http://genome.ucsc.edu/). A repetitive region within intron 2, which contained fragment length polymorphism between C57BL/6 and C3H/HeJ mice, was identified. PCR products amplified from genomic DNA of C57BL/6 and C3H/HeJ mice that contained this region were sequenced, and the polymorphism was confirmed. The primer sequences and the conditions for each PCR reaction are described in Supplementary Table 1. PCR products were resolved using a capillary electrophoresis system HAD-GT12 Genetic Analyzer (eGene Inc., Irvine, CA, USA) or by 3% NuSieve agarose (3:1) gel electrophoresis (FMC, Rockland, MA, USA).

2.3. RT-PCR analysis

Total RNA was extracted from tumor tissues using the acid guanidinium thiocyanate–phenol-chloroform method [24], and the cDNA was reverse transcribed using 10 μg total RNA, Moloney murine leukemia virus reverse transcriptase (Toyobo Co., Ltd., Osaka, Japan), and random hexamers (Takara Bio) according to the manufacturer's recommendations. The primer sequences and the conditions for each PCR reaction are described in Supplementary Table 1. PCR products were resolved by 2% agarose gel electrophoresis and analyzed using a Luminescent image analyzer LAS-3000 (Fujifilm, Tokyo, Japan). PCR products were directly sequenced using a Big Dye Terminator v3.1 (Applied Biosystems, Foster City, CA, USA) and an ABI PRISM 3100 Genetic Analyzer (Applied Biosystems) or sequenced after TA cloning using a TOPO TA cloning kit (Invitrogen Co., Carlsbad, CA, USA).

2.4. Bisulfite sequencing analysis

Genomic DNA (1.0 μg) was subjected to bisulfite modification using a CpGenome DNA modification kit, No. S7820 (Chemicon, Temecula, CA, USA), according to the manufacturer's instructions. Bisulfite-modified DNA (40 ng/μl) was then subjected to PCR amplification using primers specific for methylated CpG cytosines as described in Supplementary Table 1. PCR products were sequenced after TA cloning.

2.5. Western blot analysis

Thymic lymphoma cells and normal thymocytes were dissolved in cell lysis buffer (Cell Signaling Technology Inc., Danvers, MA, USA) containing phenylmethanesulfonyl fluoride. Proteins were denatured by heating at 100 °C for 5 min in sample buffer containing SDS, and then lysates (20 μg) were separated by 10% SDS-PAGE and transferred to a PVDF membrane (Millipore Co., Billerica, MA, USA). Anti-Pten, anti-Akt, anti-phospho-Akt (Ser473) and anti-beta-actin (Santa Cruz Biotechnology Inc., Santa Cruz, CA, USA) were used as primary antibodies. Horseradish peroxidase-conjugated anti-rabbit (Cell Signaling Technology) or anti-goat (Santa Cruz Biotechnology) IgG was used as secondary antibody. Signals were developed using ECL plus Western Blotting Detection Reagents (GE Healthcare, Little Chalfont, Buckinghamshire, UK) and analyzed using the LAS-3000 luminescent image analyzer (Fujifilm).

2.6. Array-CGH analysis

We designed and used an Agilent 8 × 15k-formatted mouse custom array-CGH microarray (#020410; Agilent Technologies, Santa Clara, CA, USA), which consisted of about 15,000 oligonucleotide probes, including 1499 for the genomic region covering the *Pten* locus on chromosome 19 (about 430 kbp). Fluorescence labeling of DNA, microarray hybridization and post-hybridization washing were carried out according to the manufacturer's protocol (version 5) for genomic DNA analysis using oligonucleotide array-CGH. Scanning was performed using an Agilent microarray scanner (G2565BA). Signal intensities were measured and evaluated using Agilent

Feature Extraction software v9-5-35 and CGH analytics software v3-5-14, respectively. The microarray data reported in this article have been deposited in the Gene Expression Ominibus (GEO) database, www.ncbi.nlm.nih.gov/geo (accession no. GSE17751).

2.7. Quantitative real-time RT-PCR

Quantitative real-time RT-PCR analysis of miR-19a and miR-21 was performed using a TaqMan MicroRNA assay kit (Applied Biosystems) according to manufacturer's recommendations. Quantitative PCR amplification of cDNAs was performed using a Mx3000P real-time PCR system (Stratagene, La Jolla, CA, USA) and TaqMan Universal PCR Master Mix (Applied Biosystems). Data were normalized to the levels of the small nucleolar RNAs 202 and 234. Each reaction was performed in triplicate. Data were analyzed with MxPro software, version 4.10 (Stratagene).

3. Results

3.1. LOH analysis

Mouse *Pten* encodes a protein product predicted to have 403 amino acid residues and is located at 24.5 cM on chromosome 19. We analyzed LOH using five independent microsatellite simple-sequence-length polymorphism makers on chromosome 19. LOH at the *Pten* locus was also examined using a microsatellite marker within intron 2, which distinguished the polymorphism between C57BL/6 and C3H/HeJ mice. LOH around the *Pten* locus was identified in seven lymphomas (TL8, 11, 12, 14, 19, 20 and 21) (Fig. 1). The LOH frequency (30%; 7 of 23 lymphomas) was roughly consistent with previous studies examining radiation-induced thymic lymphomas in various F1 hybrid mouse strains [22,23,25].

3.2. Expression of Pten mRNA and protein

We examined the expression of *Pten* transcripts by reverse transcriptase (RT)-PCR analysis using three sets of primers (Fig. 2). Altered expression of *Pten* mRNA was observed in 5 of 23 lymphomas (TL5, 8, 11, 14 and 20). TL5 had an additional but faint PCR product that was larger than the predicted product when amplified using primers Ex2F and Ex7R. For TL8, RT-PCR products generated using any primer combination were faint or undetectable. LOH at the *Pten* locus in TL8 indicated that one *Pten* allele remained. Thus the absence of *Pten* transcripts suggested the transcriptional silencing at the *Pten* promoter region in the remaining allele. Using the Ex1F-7R primer pair, TL11 generated one RT-PCR product of the predicted length and three longer RT-PCR products; TL14 generated a faint, short RT-PCR product in addition to a product of the predicted length. TL20 generated a faint product when primers Ex1F and Ex7R were used, but a substantial amount of product was generated using either of the remaining two sets of primers, suggesting that a 5′ portion of exon 1 was missing.

3.3. Sequencing of bisulfite-modified DNA

Because our data for TL8 implicated transcriptional silencing of *Pten* (Figs. 1 and 2), we analyzed the DNA methylation pat-

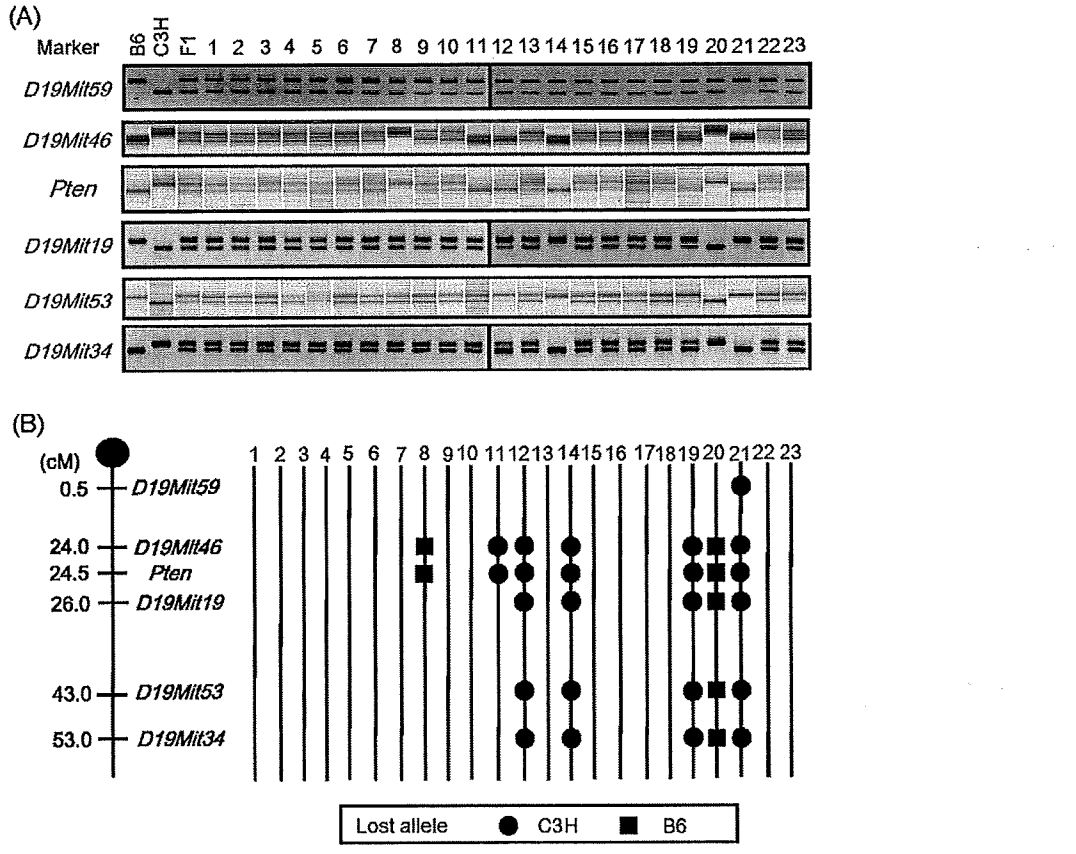

Fig. 1. LOH analysis of chromosome 19 in 23 radiation-induced thymic lymphomas. (A) The first three lanes represent control DNA samples from the maternal C57BL/6 strain (B6), the paternal C3H/HeJ strain (C3H), and the B6C3F1 hybrid (F1), respectively. Numbers above the remaining lanes reflect the tumor identification numbers. PCR amplification of genomic DNA was performed using the indicated polymorphic marker primer pair followed by electrophoretic analysis of amplification products. (B) Schematic diagram of LOH on chromosome 19 in each lymphoma. Lymphoma identification numbers are indicated at top. Polymorphic markers are shown to the right of the chromosome schematic, and marker positions indicating distances (cM) from the centromere are shown at left. The *Pten* marker is located between exons 2 and 3. Absence of a circle or square indicates the retention of heterozygosity.

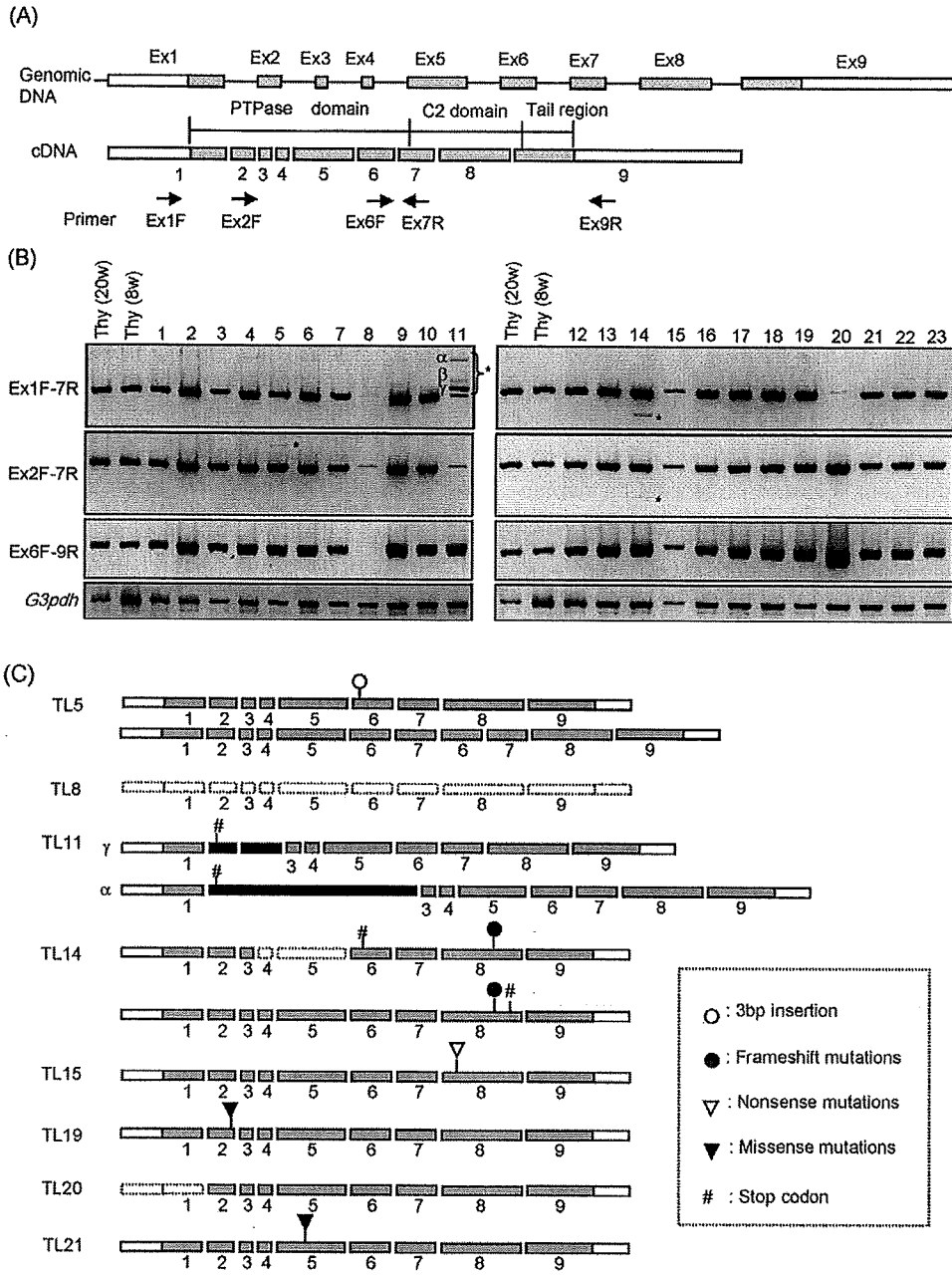

Fig. 2. Alteration of *Pten* in radiation-induced thymic lymphomas. (A) Schematic representation of *Pten*. Shading indicates the *Pten* coding regions. RT-PCR amplification primers and their annealing locations are indicated by arrows. Ex, exon; PTPase, phosphotyrosine protein phosphatase. (B) RT-PCR analysis of *Pten* using the primer pairs indicated at left and genomic DNA isolated from thymocytes (Thy) of 20- or 8-week-old mice (control lanes 1 and 2, respectively), or from the lymphoma indicated at top, was performed and reaction products were subjected to 2% agarose gel electrophoresis. *G3pdh* was used as a control for RT-PCR amplification and as a loading control. Asterisks indicate RT-PCR products longer or shorter than the expected size. (C) Schematic representation of aberrant *Pten* transcripts. Black bars in TL11 indicate inserted intronic sequences. #, Positions of newly generated in-frame stop codons that possibly cause immature translation.

terns in the 5′ (upstream) region of *Pten* (Supplementary Fig. 1A, indicated as P1) in all lymphomas; this region corresponds to the promoter of human *PTEN* that was shown to be aberrantly methylated in T-cell ALLs [26]. However, no aberrant methylation was detected (Supplementary Fig. 1B). Although the CpG sites at positions -39 and -40 relative to the transcriptional start site were both methylated in most of the lymphomas, these CpG sites were also frequently methylated in normal thymocytes. For TL8, we analyzed an additional *Pten* region (Supplementary Fig. 1A, indicated as P2) in which hypermethylation has been suggested to be associated with a lack of *PTEN* expression in non-small cell lung cancer [27]. However, we again did not detect aberrant methylation (Supplementary Fig. 1C). Thus, the absence of *Pten* transcripts likely resulted from a mechanism other than silencing by DNA methylation.

3.4. Sequence analysis of Pten transcripts

Next, we determined the sequence of the RT-PCR products from all lymphomas including those products that were longer or shorter than predicted in TL5, 11 and 14 (Fig. 2C). In TL5, the longer

PCR product generated using the Ex2F-7R primer pair contained duplicated exons 6 and 7. The product of predicted length had an insertion of 3 bp, which encoded an amino acid change from Ser170 to Met and Cys. Because the normal *Pten* sequence was not observed, TL5 may contain biallelic *Pten* mutations. TL11 had one RT-PCR product of predicted length and three longer products when amplified using the Ex1F-7R primer pair. The most predominant longer fragment generated from TL11 (Fig. 2B, indicated as γ) contained two large nucleotide insertions of 88 and 122 bp within intron 1 that generated a stop codon, together with a deletion of exon 2. The least predominant longer fragment generated from TL11 (Fig. 2B, indicated as α) contained a 1078-bp insertion in intron 1 and a deletion of exon 2, generating a stop codon. Sequencing of the TL11 PCR product β could not be achieved. The faint product of predicted length had no mutations but may have been derived from contamination of the tumor sample with healthy cells. In TL14, the predominant product of predicted length generated using the Ex6F-9R primer pair had a frameshift mutation due to a 1-bp insertion (962insA) in the poly(A)6 stretch in exon 8, creating a downstream stop codon. The faint/short PCR product of TL14, generated using either Ex1F-7R or Ex2F-7R primer pairs, had both the frameshift mutation and loss of exons 4 and 5, the latter of which generated a stop codon at residue 264. TL15 had an allele with a *Pten* nonsense mutation owing to a substitution (base 862G to T) in addition to a wild-type allele. TL19 had a *Pten* missense mutation owing to a substitution (base 158T to C), resulting in V53A. TL19 generated both mutated and wild-type PCR products, coincident with incomplete allelic LOH in TL19 (Fig. 1A). TL20 expressed only a single *Pten* transcript that lacked exon 1. TL21 had a missense mutation (base 364A to T) in *Pten*, resulting in I122F.

Overall, *Pten* transcripts in radiation-induced lymphomas had a variety of genetic lesions including missense mutations (TL19 and 21), nonsense mutations (TL15), 1- and 3-base insertions (TL14 and 5, respectively), partial intron insertions (TL11), exon duplication (TL5), exon deletion (TL11, 14, 20), and null expression (TL8). Although these mutations are very complicated, they were in good agreement with previous reports demonstrating that missense mutations occur in the Pten phosphatase domain whereas nonsense and frameshift mutations, resulting in protein truncation, occur in the C2 domain of Pten. In total, seven of eight lymphomas carrying a *Pten* mutation (88%) contained biallelic alterations.

3.5. Array-based comparative genomic hybridization (array-CGH) analysis of genomic DNA from TL8, 11 and 20

In order to know the reason for the absence or aberrant transcription of *Pten* in TL8, 11 and 20 (Fig. 2), we analyzed genomic structures around the *Pten* locus in TL8, 11 and 20 using array-CGH, which was designed for intensive analysis of the *Pten* locus. As shown in Fig. 3, the array-CGH profiles suggested partial homozygous deletions (<30 kbp) in the *Pten* locus in these lymphomas, which were positioned within the regions of hemizygous deletion in TL8 and 11. A region of homozygous deletion (~24 kbp) in TL8 occurred in the 5′ (upstream) region of *Pten*, encompassing both the putative promoter region and the transcription initiation site; this may account for the *Pten* silencing observed in TL8 (Fig. 2). Two RT-PCR products from TL11 had a deletion of exon 2 together with one or two insertion(s) of a partial sequence of intron 1 (Supplementary Fig. 2). Array-CGH indicated that TL11 had a homozygous deletion that extended 1 kbp downstream of exon 1 into the 5′ flanking region of exon 2, suggesting that the abnormal transcripts were generated by aberrant splice-site selection likely resulting from the absence of correct splice sites at the intron 1/exon 2 boundary. Array-CGH analysis of TL20 also revealed homozygous deletion of genomic regions (~4 kbp), including both the putative promoter region and the *Pten* transcription initiation site. RT-PCR analysis

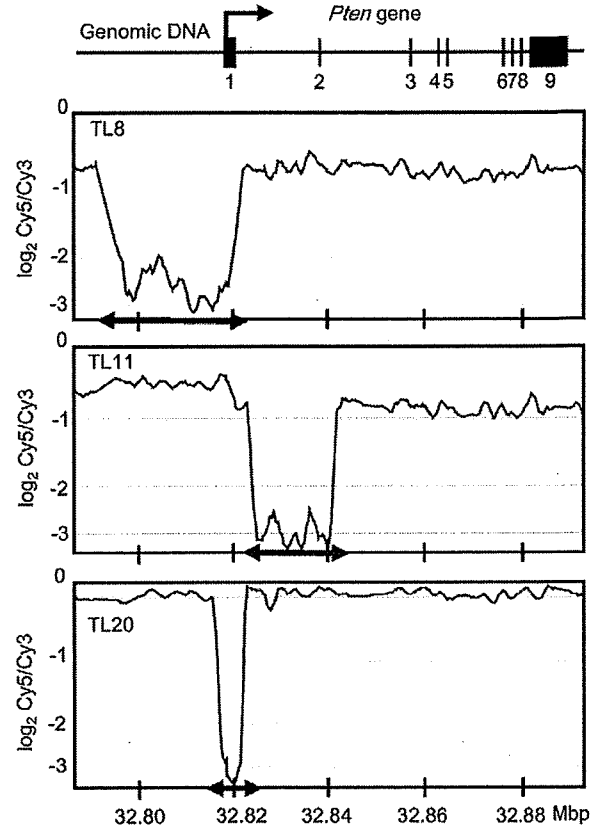

Fig. 3. Array-CGH analysis reveals homozygous focal deletions in three radiation-induced thymic lymphomas (TL8, 11 and 20). Schematic of *Pten* (top), in which shaded bars represent exons aligned to the genomic positions on chromosome 19 indicated along the *x*-axis in the array-CGH profiles below the schematic. Moving averages of the normalized $\log_2$ Cy5/Cy3 ratio, calculated based on 10 data points, are plotted in the array-CGH profiles. Arrows on the *x*-axis correspond to genomic regions amplified by PCR and sequenced to identify breakpoints.

indicated the presence of a *Pten* transcript, however, suggesting that the ectopic transcription was initiated at a cryptic promoter in TL20.

To explore the mechanism responsible for these deletions, genomic regions containing the breakpoints (indicated by the *x*-axis arrows in Fig. 3) were amplified by PCR and sequenced (Fig. 4), which identified nucleotide insertions at the breakpoint junctions in TL8 and 11. In TL11, a pair of recombination signal sequence-like sequences, composed of heptamer- and nonamer-like motifs separated by non-conserved spacers of 12 or 23 bp, were located between but immediately adjacent to the breakpoints, suggesting that illegitimate V(D)J recombination gave rise to the deletion. In contrast, a 0.8-kb templated nucleotide sequence was inserted in the TL20 deletion region. Overlaps of 1 or 2 nucleotides at both breakpoints of the two junctions were identified, suggesting that microhomology-mediated rearrangements might have led to the deletion.

3.6. Loss of Pten and downstream activation of Akt

Pten protein expression varied in the lymphomas we examined (Fig. 5). To determine whether decreased expression correlated with loss of Pten function, we analyzed the degree of Ser473 phosphorylation in Akt (Fig. 5). Pten was not expressed in lymphomas TL8, 11, 14 and 20, consistent with the aberrant stop codon and genomic deletions in the *Pten* promoter region. Pten expression level correlated inversely with phosphorylation of Akt. Lymphomas